



# Silicon might mitigate nickel toxicity in maize roots via chelation, detoxification, and membrane transport

Olha Lakhneko<sup>a</sup>, Ivana Fialová<sup>a</sup>, Roderik Fiala<sup>a</sup>, Mária Kopáčová<sup>b</sup>, Andrej Kováč<sup>c</sup>, Maksym Danchenko<sup>a,\*</sup>

<sup>a</sup> Plant Science and Biodiversity Centre, Slovak Academy of Sciences, Bratislava 84523, Slovakia

<sup>b</sup> Institute of Chemistry, Slovak Academy of Sciences, Bratislava 84538, Slovakia

<sup>c</sup> Institute of Neuroimmunology, Slovak Academy of Sciences, Bratislava 84510, Slovakia

## ARTICLE INFO

### Keywords:

Glycine betaine  
Heavy metal  
Mineral amendment  
Proteome  
Soluble sugars  
*Zea mays*

## ABSTRACT

Nickel is an essential micronutrient for plant growth and development. However, in excessive amounts caused by accidental pollution of soils, this heavy metal is toxic to plants. Although silicon is a non-essential nutrient, it accumulates in most monocots, particularly the vital crop maize (corn, *Zea mays*). In fact, this metalloid mineral can alleviate the toxicity of heavy metals, though the mechanism is not entirely clear yet. Herein, we measured proteome, gene expression, enzyme activities, and selected sugars to investigate such effect thoroughly. Deep proteomic analysis revealed a minor impact of 100  $\mu\text{M}$  Ni, 2.5 mM Si, or their combination on roots in 12-day-old hydroponically grown maize seedlings upon 9 days of exposure. Nonetheless, we suggested plausible mechanisms of Si mitigation of excessive Ni: Chelation by metallothioneins and phytochelatins, detoxification by glycine betaine pathway, and restructuring of plasma membrane transporters. Higher activity of glutathione S-transferase confirmed its plausible involvement in reducing Ni toxicity in combined treatment. Accumulation of sucrose synthase and corresponding soluble sugars in Ni and combined treatment implied high energy requirements both during heavy metal stress and its mitigation. Expression analysis of genes coding a few differentially accumulated proteins failed to reveal concordant changes, indicating posttranscriptional regulation. Proposed mitigation mechanisms should be functionally validated in follow-up studies.

## 1. Introduction

The global threat of soil nickel pollution draws the attention of investigators. This heavy metal leaks into the environment from different natural sources (such as, bedrock weathering and volcano eruptions) and various anthropogenic activities (e.g., agricultural fertilization and pesticides or industrial wastes) (Mustafa et al., 2023). Excessive Ni concentration in soil is harmful to plant physiological processes; for example, it impairs photosynthetic efficiency. (Sheoran et al., 1990). Nickel triggers the accumulation of a large amount of reactive oxygen species (ROS); however, its toxicity is primarily connected to the inhibition of antioxidative enzyme activities rather than the formation of ROS (Amjad et al., 2020; Shahzad et al., 2018). If present in soil over 35 mg kg<sup>-1</sup>, Ni is toxic to all living organisms (El-Naggar et al., 2021). The legislation on the limits of heavy metals is country-specific. Frequently referenced Finnish Decree defines soil contamination by Ni over 100–150 mg kg<sup>-1</sup> with a threshold value for detailed monitoring

over 50 mg kg<sup>-1</sup> (Ministry of the Environment, Finland, 2007; van der Voet et al., 2013). Recent data indicates that Ni contaminates the majority of European Union soils to some extent, yet the highest frequency of dirty samples is in Greece (Tóth et al., 2016).

On the other hand, Ni is an essential micronutrient for plant growth and development. As a part of metalloenzymes, it is vital for secondary metabolism rather than primary one (Wood, 2015). Nickel is an irreplaceable part in the active site of urease (EC 3.5.1.5, urea amidohydrolase), which catalyzes the hydrolysis of urea to ammonium and bicarbonate and thus participates in nitrogen metabolism predominantly when urea is the source (Dixon et al., 1975; Ragsdale, 2009). It is still the only proven nutritional function of Ni in higher plants. Only a few plant species can normally grow and develop without Ni (Gerendás et al., 1999).

Silicon is a highly abundant element on our planet. It is considered a non-essential nutrient for plant growth and development. Nonetheless, it is present in a variable amount in a vast majority of plants (Cooke and

\* Correspondence author.

E-mail address: [maksym.danchenko@savba.sk](mailto:maksym.danchenko@savba.sk) (M. Danchenko).

<https://doi.org/10.1016/j.ecoenv.2024.117334>

Received 5 August 2024; Received in revised form 23 October 2024; Accepted 10 November 2024

Available online 16 November 2024

0147-6513/© 2024 The Author(s). Published by Elsevier Inc. This is an open access article under the CC BY license (<http://creativecommons.org/licenses/by/4.0/>).

Leishman, 2011; Mir et al., 2022; Zargar et al., 2019). Plants can be classified as accumulators and excluders, in relation to Si in soil. Monocots, particularly grasses, like rice (*Oryza sativa*), wheat (*Triticum aestivum*), or maize (corn, *Zea mays*), predominantly accumulate a substantially larger amount of Si in their tissues, while dicots are mostly unable to accumulate it and belong to excluders (Deshmukh et al., 2015, 2013).

Despite Si is a non-essential metalloid element and plants can normally survive in its absence, numerous works proved the positive effect of this mineral supplement on plant metabolism. Moreover, its presence in the environment can improve the growth and development of accumulator plants under adverse, both abiotic and biotic conditions (Mir et al., 2022; Ranjan et al., 2021; Song et al., 2016; Xie et al., 2015). Particularly, Si accumulators can benefit significantly from its presence in soil under heavy metal stress. The authors showed that Si reduced the uptake of heavy metals by plant roots. It formed silicate complexes with metals in the soil, making them less bioavailable, thus minimizing the accumulation of toxic metals in plant tissues (Cocker et al., 1998; Gu et al., 2011). Silicon can enhance the natural tolerance mechanisms against heavy metal stress. It may improve antioxidant defense, including the activity of enzymes, which scavenge ROS produced under metal stress (Adrees et al., 2015; Fiala et al., 2021; Rahman et al., 2023). Silicon treatment resulted in the expression of specific transporters and genes associated with photosynthesis. They apparently participate in the plant adaptive response to heavy metal stress (Adrees et al., 2015; Kim et al., 2014). While Si mitigated heavy metal stress in some plants, further research is needed to fully understand the underlying mechanisms and propose practical solutions for agriculture.

Maize is an essential crop significant for different aspects of human life: Food source, livestock feed, industrial biofuel, and manufacturing material (FAO 2022). Its annual production exceeds one billion tons (Erenstein et al., 2022). Heavy metal pollution seriously compromises maize growth and yield (Romdhane et al., 2021). Moreover, the high ability of maize to bioaccumulate heavy metal cations from the environment restricts its further food usage (Abbas et al., 2023; Amjad et al., 2020; Ruiz-Huerta et al., 2022). Researchers showed that Si can improve stress-related parameters in maize during metal stress (Fiala et al., 2021; Vaculík et al., 2015, 2021).

Earlier, we demonstrated that Si indeed mitigated Ni stress predominantly by regulating the level of enzymatic and non-enzymatic antioxidants in maize roots and leaves (Fiala et al., 2021). Herein, we focused on roots—gates to the incoming heavy metals—first to contact adverse conditions. We aspired to clarify the biochemical mechanism of an alleviating effect during the combined application of Ni and Si. Accordingly, we compared root proteomic profiles complemented by gene expression analysis, enzymatic assays, and evaluation of soluble sugars content.

## 2. Materials and methods

### 2.1. Plant material and growth conditions

We investigated seeds of the maize hybrid Valentina (provided by RWA Slovakia). The experimental setup was described earlier (Fiala et al., 2021). Briefly, surface sterilized seeds were germinated for 3 days in darkness at 26 °C. Then, control seedlings were grown in Hoagland solution under controlled conditions: Light/dark 16/8 h, temperature 24/22 °C, relative humidity 60 %, and light intensity 180  $\mu\text{mol m}^{-2} \text{sec}^{-1}$  of photosynthetically active radiation. Nickel treatment comprised an additional 100  $\mu\text{M}$  Ni ( $\text{NiCl}_2 \times 6 \text{H}_2\text{O}$ ). Silicon treatment included 2.5 mM Si (27 %  $\text{SiO}_2$  in 14 % NaOH). An alleviating effect was observed by adding both 100  $\mu\text{M}$  Ni and 2.5 mM Si. The pH of the nutrient solution was adjusted to 6.2 with HCl, and the exposure lasted for 9 days. Then, the apical segments of roots were collected, rapidly frozen in liquid nitrogen, and stored at  $-70^\circ\text{C}$  until analyzed.

### 2.2. Sample preparation for the discovery proteomics

Aliquots of frozen root tips (100 mg fresh weight) were crashed in plastic tubes by a bead-beating homogenizer cooled with liquid nitrogen. Proteins were isolated using phenol extraction protocol with ammonium acetate precipitation, as described in the literature (Isaacson et al., 2006). The final pellets, containing purified proteins, were solubilized in buffer with detergent 4 % SDS, 100 mM Tris pH 7.6, and 100 mM dithiothreitol. Consequently, protein concentrations were estimated by Pierce reducing agent-compatible BCA assay (Thermo Scientific, MA, USA). Proteins were profiled by conventional 12 % SDS-PAGE to verify the quality and consistency of extracts across replicates and treatments.

Total protein extracts (50  $\mu\text{g}$ ) adjusted to 200  $\mu\text{L}$  with urea buffer (8 M urea in 50 mM ammonium bicarbonate) were digested with trypsin using filter-aided sample preparation on Microcon Ultracel YM-10 centrifugal filters (Sigma-Aldrich, MO, USA) (Distler et al., 2016). Before digestion, the filters were washed with 50 mM ammonium bicarbonate. Samples were incubated overnight at 37 °C with trypsin gold (Promega, WI, USA) in the proportion 1:50 to total proteins and slightly acidified by a few drops of 10 % trifluoroacetic acid. Consequently, the peptide mixtures were purified on SEP PAK C18 light columns (Waters, UK) and vacuum-concentrated. The concentration of peptides was measured spectrophotometrically by nanoDrop 2000 (Thermo Scientific, MA, USA) and adjusted to 100  $\text{ng } \mu\text{L}^{-1}$  with 0.1 % trifluoroacetic acid.

### 2.3. Relative label-free quantification

Complex peptide mixtures (300 ng) were separated using Acquity M-Class UHPLC (Waters, UK). Firstly, samples were desalted and concentrated on the nanoEase Symmetry C18 trap column (20 mm length, 180  $\mu\text{m}$  diameter, 5  $\mu\text{m}$  particle size) (Waters, UK). Secondly, peptides were comprehensively profiled on the nanoEase HSS T3 C18 analytical column (250 mm length, 75  $\mu\text{m}$  diameter, 1.8  $\mu\text{m}$  particle size) (Waters, UK) using a 90 min gradient of 5–35 % acetonitrile with 0.1 % formic acid at a flow rate of 300  $\text{nL min}^{-1}$ . Next, samples were nanosprayed by PicoTip emitter (New Objective, MA, USA) with 2.9 kV capillary voltage to the quadrupole time-of-flight mass spectrometer Synapt G2-Si (Waters, UK). The instrument with enabled ion mobility, which provided additional gas-phase separation of ions, was tuned using parameters described in the literature (Distler et al., 2016). Spectra were recorded in a data-independent mode, high-definition MSE. Ions with 50–2000  $\text{m z}^{-1}$  were detected in both low-energy and high-energy channels. The external standard Glu1-Fibrinopeptide B was infused for mass correction.

Compression and Archival Tool 1.0 (Waters, UK) reduced noise, removing ion counts below 15. Subsequent processing was done in Progenesis QI 4.1 (Waters, UK). Peaks were modeled with a low energy threshold 400 counts and a high energy threshold 40 counts. Chromatographic elution profiles in low- and high-energy traces were correlated to assign fragment ions to appropriate precursor ions. The retention times of peaks were aligned to an automatically selected reference chromatogram. Next, peak intensities were normalized to the median distribution of all ions. The label-free quantification relied on integrating peak areas of the three most intense precursor peptides. Arcsinh transformation of data was done before statistics. We used Ion Accounting 4.0 (Waters, UK) search algorithm for protein identification. Spectra were searched against maize proteome sequences downloaded from UniProt in November 2019 (99,253 entries, uniprot.org). Search parameters were: (i) one trypsin miscleavage, (ii) fixed carbamidomethyl cysteine, (iii) variable oxidized methionine, (iv) automatic mass tolerance, (v) 4 % false discovery rate against the randomized database. Protein hits having unique peptides were accepted if at least two reliable peptides (score  $\geq 5.81$ , mass accuracy  $\leq 20$  ppm) matched the sequence.

## 2.4. RNA isolation and qPCR

RNA was isolated from the 50 mg root sample using RNeasy Plant Mini Kit (Qiagen, Germany). Subsequently, 1 µg of the total RNA sample was treated by DNase I, RNase-free (Thermo Scientific, MA, USA). cDNA synthesis was performed using FIREScript RT cDNA synthesis Kit (Solis BioDyne, Estonia). qPCR reaction mixture contained FastStart SYBR Green Master (Roche, Switzerland), gene-specific forward and reverse primers 0.5 mM each (Microsynth AG, Switzerland), and 10 % of the final volume of cDNA sample. Primer sets for the selected genes were designed, and their specificity was checked using Primer-BLAST, ncbi.nlm.nih.gov/tools/primer-blast/ (Table S1). The 3-stage qPCR reaction (95 °C 10 s, 52/58/60 °C 20 s, 72 °C 20 s, 45 cycles) was run in Light-Cycler 96 System (Roche, Switzerland). The amplification was validated at the melting stage; only results providing a single peak were considered. The coefficient of amplification efficiency for each pair of primers was determined by 3-fold serial dilutions, and primers with an efficiency 90–115 % were considered. Gene expression was calculated using four biological and three technical replicates through Pfaffl equation (Pfaffl, 2001). Three reference genes, elongation factor 1- $\alpha$ ,  $\beta$ -tubulin 7, and cyclophilin (Y. Lin et al., 2014), were used for normalizing qPCR data based on the geometric mean (Vandesompele et al., 2002).

## 2.5. Enzymatic activity assays

For glutathione S-transferase (GST) activity measurement, the crude extract was prepared using 25 mg of fine homogenized root powder mixed with 300 µL of extraction buffer (0.1 M phosphate buffer pH 7, 1 mM PMSF, and 1 % PVPP). Glutathione S-transferase activity was determined by binding with 1-chloro-2,4-dinitrobenzene (CDNB). The change in absorbance was measured at 340 nm ( $\epsilon_{340} = 9.6 \text{ mM}^{-1} \text{ cm}^{-1}$ ) for 5 min using microplate reader Synergy H (Agilent, CA, USA) immediately after adding the CDNB to the reaction mixture (Czékus et al., 2020).

For lipoxygenase (LOX) activity measurement, the crude extract was obtained from 25 mg of root tissue in 50 µL of bidistilled water. The debris was separated by centrifugation at  $12,500 \times g$  for 15 min, 4 °C. Lipoxygenase activity was measured by mixing 1 µL of crude extract, 200 µL 50 mM sodium phosphate buffer pH 7.0, and 5 µL 10 mM linoleic acid emulsified in 0.36 % Tween-20 (Marenco et al., 1995). The change in absorbance at 234 nm ( $\epsilon_{234} = 25 \text{ mM}^{-1} \text{ cm}^{-1}$ ) was recorded immediately after adding linoleic acid and after 10 min. Enzymatic activities were calculated relative to protein content in extracts measured employing Pierce Bradford protein assay (Thermo Scientific, MA, USA).

## 2.6. Carbohydrate content estimation

The fresh samples of the maize roots were lyophilized in freeze-dryer Beta 2–8 LSCplus (Christ, Germany) for 48 h. Next, the samples were weighted and extracted with 50 % methanol in the 2 mg mL<sup>-1</sup> proportion. The samples were sonicated with Sonorex TK 22 (Bandelin, Germany) for 5 min, vortexed, and extracted overnight. Then, 300 µL of each extract was transferred into the vial and evaporated in block heater SBH130D (Stuart, UK). The dried extracts were derivatized by trimethylsilylation (TMS) with 100 µL Silylating mixture I according to Sweeley (Sigma-Aldrich, MO, USA) by incubation in a block heater at 80 °C for 30 min. After the vials cooled down, chloroform was added to 1 mL. Per-O-acetyl-arabitol (arabitol pentaacetate, Carbosynth, UK) was chosen as an internal standard because it was acetylated, undetectable in the extracts, did not increase the run time or interfere with the peaks of TMS fructose, glucose, myo-inositol, and sucrose. An aliquot of 5 µL of 10 mg mL<sup>-1</sup> internal standard was added into each vial with extract and vortexed.

Samples were analyzed by gas chromatography coupled with mass spectrometry (GC-MS) on ITQ 900 (Thermo Scientific, MA, USA) with electron ionization using standard 70 eV electron energy, emission

current 25 µA, and ion source temperature 200 °C. Trace GC Ultra (Thermo Scientific, MA, USA) was equipped with a TG-SQC capillary column containing 5 % phenyl methylpolysiloxane (30 m length,  $\times$  0.25 mm diameter,  $\times$  0.25 µm particle size) (Thermo Scientific, MA, USA). Helium with flow rate 0.4 mL min<sup>-1</sup> was used as mobile phase, and the temperature program was: 4 min at 80 °C, 8 °C min<sup>-1</sup> to 160 °C (4 min hold), 4 °C min<sup>-1</sup> to 250 °C (15 min hold). External standards of targeted compounds (fructose, glucose, myo-inositol, and sucrose, all Carbosynth, UK) were prepared as described above with TMS derivatization (200 µL of Silylating mixture I). The compounds were identified in samples, comparing the mass spectra and retention times with standards. The quantified areas of the compounds in samples were converted according to the coefficients of areas of the same amount of internal standard and corrected for external standards.

## 2.7. Statistical analysis and visualization

Statistical analysis of non-proteomic data was done in Prism 9.3 (GraphPad, CA, USA) using ANOVA followed by Tukey's posthoc test. Proteomic data were evaluated in Perseus 1.6.15 (maxquant.net/perseus/) with the same statistical tests. Additionally, a principal component analysis was done. Next, we performed hierarchical clustering on Z-score normalized means with Euclidean distance and k-means preprocessing.

## 3. Results and discussion

Proteome profiling of corn roots allowed the identification and quantification of 3545 proteins (Table S2a). However, only 47 of them were differentially abundant (ANOVA  $P \leq 0.05$ ) with effect size at least 50 % across all experimental treatments, indicating a minor effect of metal, mineral, and their combination (Table S2b). The principal component analysis confirmed sufficient reproducibility within the dataset (Fig. 1a). Differentially abundant proteins were grouped in 3 clusters: (i) 'Ni high'—24 proteins; (ii) 'Ni low'—17; and (iii) 'Ni high, Si low'—6 (Fig. 1b and S1). Though, these clusters are somewhat heterogeneous, such as a few proteins deviate from a characteristic abundance pattern.

### 3.1. Role of proteins with higher abundance upon nickel application

#### 3.1.1. Primary metabolism

The cluster 'Ni high' contains the substantial part of differentially accumulated proteins with the highest effect size (Fig. 1b, Table 1 and S2b). A0A1D6GWZ6 sucrose synthase (SuSy) in Ni+Si roots had a 29.0-fold increase ( $P = 0.0198$ ), and in Ni-treated samples had an 18.8-fold increase ( $P = 0.0707$ ) both versus control. Sucrose synthase (EC 2.4.1.13) is a glycosyl transferase that reversibly cleaves sucrose into fructose and glucose (uridine diphosphate glucose or adenosine diphosphate glucose) in sink tissues. Cell wall and plasma membrane SuSy produces uridine diphosphate glucose for subsequent synthesis of cellulose and callose (Stein and Granot, 2019). Arsenate toxicity increased the activity of SuSy in the roots of rice seedlings and both reducing and non-reducing sugar content (Choudhury et al., 2010). Cadmium treatment did not affect hydrolyzing SuSy activity, but SuSy synthesizing activity declined with increasing amount of cadmium in 18-day-old maize roots (Li et al., 2020); furthermore, enzyme synthesizing activity declined only in a sensitive hybrid of maize at earlier treatment points (Li et al., 2022). Another study with cadmium treatment pointed to a variable change of SuSy activity in the roots of pea (*Pisum sativum*)—increase on the 3rd day, decrease on the 5th day, and no changes on the 7th day of treatment (Devi et al., 2007). B4FFZ9 oil body-associated protein 1 A had a 2.2-fold higher abundance in Ni ( $P = 0.0832$ ) and 3.2-fold higher abundance in Ni+Si ( $P = 0.0105$ ) both compared to the control. Oil body proteins cover specialized organelles, protecting them from aggregation and regulating their size (Shao et al.,

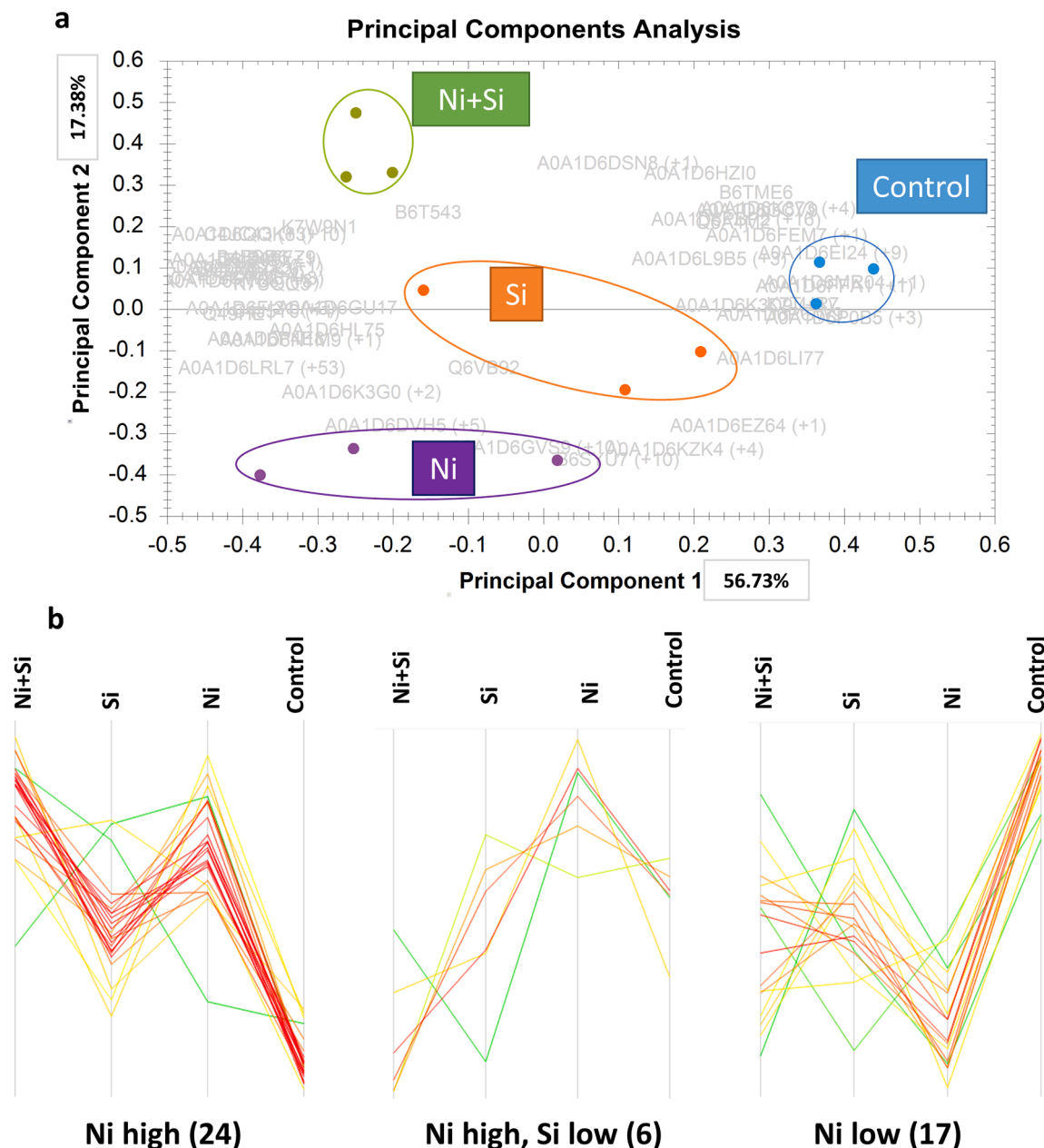


**Fig. 1.** Multidimensional statistical analysis of 47 differentially abundant proteins in roots of 12-day-old hydroponically grown maize seedlings after 9 days of treatment: (a) Principal component analysis, and (b) accumulation profile within clusters. The experiment was conducted in 3 biological replicates. Hierarchical clustering was performed on Z-score normalized means with Euclidian distance. Clusters were semantically named based on the similarity of accumulation profiles. Ni refers to 100  $\mu$ M Ni treatment, and Si refers to 2.5 mM Si treatment.

2019; Shimada and Hara-Nishimura, 2010). Oil body-associated proteins class 1 are typically anchored with a hairpin in the endoplasmic reticulum membrane and laterally diffuse until entering an emerging oil body. Lipid-depositing organelles relieve endoplasmic reticulum stress by correcting the lipid composition of its membrane and maintaining protein homeostasis (Olzmann and Carvalho, 2019). The authors reported an increased accumulation of oil bodies in cells of cadmium-stressed roots of pea (Głowacka et al., 2019). Though there is no clear evidence of an oil body-mediated defense mechanism in plants in the presence of toxic metal, theories appeared for yeast and protozoa (Morón et al., 2022; Rajakumar et al., 2020). A0A1D6M6Z2 NADH-cytochrome b5 reductase (EC 1.6.2.2) accumulated 3.8-fold in Ni+Si samples against control ( $P = 0.0279$ ). This protein desaturates and hydroxylates fatty acids (Liu, 2022). The authors showed that NADH-cytochrome b5 reductase plays an important role in ATP

production and increasing levels of polyunsaturated fatty acids during osmotic stress (Xiao et al., 2023). A0A1D6HL75 chloroplastic ferredoxin-nitrite reductase accumulated 2.5-fold in Ni and Ni+Si compared to the control ( $P = 0.0582$  and  $P = 0.0635$ , respectively). This protein (EC 1.7.7.1) catalyzes nitrite reduction to ammonium in the nitrogen metabolism (Sanz-Luque et al., 2015). Nitrite reductase activity is typically lower under heavy metal stress (Dinakar et al., 2009; Ghosh et al., 2013). It will be interesting to explore the direct functional relevance of SuSy and oil body-associated protein 1 A in Si protection from Ni toxicity using knockout and overexpressor lines.

### 3.1.2. Metallothioneins and phytochelatins

P43401 EC (early cysteine-labeled) protein class II or zinc-containing metallothionein had a massive 15.5-fold higher abundance in Ni+Si compared to control ( $P = 0.0345$ ), and a 7.2-fold increase in Ni against



**Table 1**  
Effect size for differentially abundant proteins.

UniProt ID	Protein name	Cluster	Si/ C	Ni/ C	Ni+Si/ C
A0A1D6GWZ6	Sucrose synthase	Ni↑	8.9	18.8	<b>29.0</b>
P43401	EC prot. homolog	Ni↑	4.3	7.2	<b>15.5</b>
A0A1D6M6Z2	NADH-cytochrome b5 reductase	Ni↑	2.0	2.9	<b>3.8</b>
Q49HE1	12-oxo-phytodienoic acid reductase	Ni↑	1.8	<b>2.5</b>	<b>2.5</b>
B4FFZ9	Oil body-associated prot. 1 A	Ni↑	1.8	2.2	<b>3.2</b>
A0A1D6GU17	Phenolic glucoside malonyltransferase 1	Ni↑	<b>1.6</b>	1.4	<b>1.5</b>
A0A1D6K3G0	DGS1 mitochondrial	Ni↑	1.5	<b>1.6</b>	1.2
A0A1D6FI21	Serine/threonine-prot. phosphatase	Ni↑	1.5	2.5	2.4
A0A1D6P4E8	Tryptophan synthase β type 2	Ni↑	1.5	<b>1.9</b>	<b>1.8</b>
A0A1D6HL75	Ferredoxin-nitrite reductase chloroplastic	Ni↑	1.5	2.7	2.5
C4JC43	Target of Myb prot. 1	Ni↑	1.5	1.7	<b>2.7</b>
A0A1D6IP09	BADH-like prot.	Ni↑	1.4	1.7	<b>2.2</b>
B6T543	Histone H2A	Ni↑	1.3	1.0	<b>1.5</b>
A0A1D6QQK8	ABC transporter A fam. member 7	Ni↑	1.3	1.8	<b>3.0</b>
Q7Y037	Calcium-dependent prot. kinase 11	Ni↑	1.3	1.6	<b>1.9</b>
B4FSR6	Glutathione S-transferase	Ni↑	1.3	1.3	<b>1.5</b>
A0A1D6HT66	Evolutionarily conserved C-terminal region 2	Ni↑	1.3	1.6	<b>1.8</b>
K7UQQ3	O-methyltransferase ZRP4	Ni↑	1.3	1.4	<b>1.5</b>
B7ZZ56	Glycosyltransferase	Ni↑	1.2	1.5	<b>1.7</b>
A9LLX9	TERMINAL FLOWER 1	Ni↑	1.2	1.5	<b>1.7</b>
A0A1D6LRL7	Pectin lyase-like fam. prot.	Ni↑	1.2	<b>1.5</b>	<b>1.3</b>
K7W9N1	Putative leucine-rich repeat receptor-like prot. kinase fam. prot.	Ni↑	1.1	1.5	<b>2.9</b>
A0A1D6EZ64	Polygalacturonase inhibitor 1	Ni↑Si↓	1.1	0.9	<b>0.5</b>
A0A1D6DVH5	Lipoxygenase	Ni↑Si↓	1.1	1.8	1.0
A0A1D6N1M9	Serine/arginine repetitive matrix prot. 2 isoform 4	Ni↑Si↓	1.0	<b>2.0</b>	1.5
A0A1D6KZK4	Cox19-like CHCH fam. prot.	Ni↑Si↓	1.0	1.1	0.6
A0A1D6LI77	Ras-related prot. RABD1	Ni↓	1.0	0.8	0.7
B6SYU7	Cox19-like CHCH fam. prot.	Ni↑Si↓	1.0	1.2	0.7
C4J5Y0	C3HC4-type RING finger prot.	Ni↑	1.0	1.9	1.8
Q6A4M2	3-ketoacyl reductase GL8B	Ni↓	0.9	<b>0.5</b>	0.8
K7TUR7	TRAF transcription factor	Ni↓	0.9	<b>0.5</b>	<b>0.5</b>
A0A1D6GVS9	Mitogen-activated prot. kinase	Ni↑Si↓	0.9	1.4	0.7
A0A1D6PBP2	Glucose—6-phosphate 1-dehydrogenase	Ni↓	0.8	<b>0.7</b>	0.8
A0A1D6PGW9	Methionyl-tRNA synthetase	Ni↓	0.8	0.6	<b>0.6</b>
A0A1D6MR04	Pentatricopeptide repeat-containing prot. mitochondrial	Ni↓	0.8	<b>0.6</b>	<b>0.6</b>
B6TME6	MICOS complex subunit Mic10	Ni↓	0.7	<b>0.6</b>	0.8
A0A1D6FEM7	Reverse transcriptase domain-containing prot.	Ni↓	<b>0.7</b>	<b>0.6</b>	<b>0.8</b>
A0A1D6DSN8	40S ribosomal prot. S4—3	Ni↓	0.7	0.5	1.1
A0A1D6P0B5	RING-type E3 ubiquitin transferase	Ni↓	0.7	<b>0.5</b>	<b>0.4</b>
A0A1D6FFA1	Enhancer of polycomb-like transcription factor prot.	Ni↓	0.7	<b>0.6</b>	<b>0.6</b>
A0A1D6HZI0	RNA-binding prot. CP31B chloroplastic	Ni↓	<b>0.6</b>	<b>0.5</b>	0.9
A0A1D6L9B5	Histidine acid phosphatase	Ni↓	<b>0.6</b>	0.7	0.7
A0A1D6K3D9	β-Adaptin-like prot.	Ni↓	<b>0.5</b>	0.6	<b>0.5</b>
Q6VB92	β-Glucanase	Ni↑Si↓	0.5	1.7	0.9

**Table 1 (continued)**

UniProt ID	Protein name	Cluster	Si/ C	Ni/ C	Ni+Si/ C
A0A1D6GCV9	EXPORTIN 1 A	Ni↓	0.5	<b>0.3</b>	0.5
A0A1D6EI24	ERAD-associated E3 ubiquitin ligase HRD1A	Ni↓	<b>0.4</b>	<b>0.3</b>	<b>0.4</b>
A0A1D6K873	3-Hydroxyisobutyryl-CoA hydrolase-like prot. 2 mitochondrial	Ni↓	<b>0.3</b>	<b>0.2</b>	0.5

**Footnote** Ni↑—‘Ni high’; Ni↓—‘Ni low’; Ni↑Si↓—‘Ni high, Si low’; C—Control; Si—2.5 mM Si treatment; Ni—100 μM Ni treatment; Ni+Si—combined exposure; fam.—family; prot.—protein. Bold ratios indicate significant differences in the respective comparison (Tukey’s test  $P \leq 0.05$ ).

control ( $P = 0.2063$ ). Metallothioneins are well-known for their role in heavy metal detoxification by chelation inside the cell (Patankar et al., 2019). Several works described elevated expression in roots and protection from heavy metal toxicity (Konieczna et al., 2023; Pan et al., 2018; Zhou et al., 2014). Apparently, plants in combined treatment synergistically accumulated EC metallothionein class II. Of note, B4FSR6 GST class τ accumulated 1.5-fold in Ni+Si compared to control ( $P = 0.0273$ ). Glutathione S-transferase (EC 2.5.1.18) catalyzes the conjugation of toxic compounds with glutathione (Chronopoulou et al., 2014). Heavy metals, including Ni, induced expression of GST genes in rice seedling roots (Lin et al., 2013). Furthermore, overexpression of GST enhanced tolerance to cadmium (Dixit et al., 2011; Liu et al., 2013). Upregulation of GST gene induced synthesis of phytochelatin for detoxification of excessive copper (Lim et al., 2005). Glutathione S-transferase detoxification might be critical for mediating the protective action of Si.

### 3.1.3. Restructuring plasma membrane transporters

A0A1D6QQK8 ABC transporter A family member abundance spiked in Ni+Si roots 3.0 times versus control ( $P = 0.0031$ ) and 2.3 times compared to Si ( $P = 0.0125$ ). ABC transporters are essential for alleviating heavy metal toxicity (Feng et al., 2020; Fu et al., 2019). Of note, each plant species may have an individual expression pattern of various types of ABC transporters under different toxic metals (Naaz et al., 2023). Accumulation during combined treatment suggests that Si activates specific routes combating Ni toxicity with a unique role of ABC transporter A. Under Ni+Si treatment, C4JC43 target of Myb protein 1 accumulated 2.7-fold against control ( $P = 0.0037$ ) and 1.9-fold against Si ( $P = 0.0404$ ). The mammalian target of Myb protein 1 (TOM1) contributes to loading the endosomal sorting complex required for transport in the cytosol (ESCRT-0) (Mosesso et al., 2019). Plant orthologue TOM1-like proteins (TOLs) show functional analogy to ESCRT-0 acting as a ubiquitin receptor and mediating vacuolar degradation of plasma membrane cargos, contributing to the regulation of protein abundance and their localization at the plasma membrane (Moulinier-Anzola et al., 2020). Still, little is known about the process, though the role in stress response was discussed (Gao et al., 2017). Higher abundance in combined exposure might indirectly reflect an active restructuring of membrane transporters, a plausible mechanism of Si mitigation effect.

### 3.1.4. Glycine betaine synthesis

A0A1D6IP09 BADH-like protein had 2.2-fold elevated abundance in Ni+Si compared to control ( $P = 0.0166$ ). Interestingly, Ni-treated plants had a non-significant increase with a lower effect size—1.7-fold ( $P = 0.1275$ ). Betaine aldehyde dehydrogenase (BADH, EC 1.2.1.8) is a key enzyme of glycine betaine synthesis, which accumulation, enabling tolerance, was reported under abiotic stresses (C. Yang et al., 2015). However, there is scarce evidence of the accumulation of glycine betaine under heavy metal stress—authors showed that cadmium but not zinc increased the level of BADH transcripts in roots of seashore mallow (*Kosteletzkya pentacarpos*) (M.-X. Zhou et al., 2019). We propose that Si amendment intensified the glycine betaine-mediated mitigation route.

### 3.1.5. Signaling and splicing

K7W9N1 putative leucine-rich repeat receptor-like protein kinase accumulated 2.8-fold during Ni+Si versus control ( $P = 0.0323$ ) and versus Si alone ( $P = 0.0314$ ). Leucine-rich repeat receptor kinases (LRR-RKs) are receptor molecules that relay signals during developmental processes and stress perception (Soltabayeva et al., 2022). They are involved in signal transduction under heavy metal stress (He et al., 2019). A0A1D6N1M9 serine/arginine repetitive matrix protein 2 isoform 4 accumulated 2-fold in Ni-treated roots ( $P = 0.0381$ ), while combined treatment lowered its abundance almost to the level of control plants. This protein is a part of the family of serine/arginine-rich proteins regulating alternative splicing (Rosenkranz et al., 2021; Xu et al., 2022). The vital role of alternative splicing proteins under abiotic stresses was already described, particularly under cadmium stress (Butt et al., 2022; Laloum et al., 2018; Ling et al., 2021). We interpret that reverted to the control level abundance of this stress-related protein in combined exposure highlights Si mitigation of Ni toxicity.

### 3.2. Role of proteins with lower abundance upon nickel application

The most significant change in cluster 'Ni low' belonged to proteins: A0A1D6DSN8 40S ribosomal protein S4–3, Q6A4M2 3-ketoacyl reductase GL8B, A0A1D6GCV9 EXPORTIN 1 A, A0A1D6K873 3-hydroxyisobutyryl-CoA hydrolase-like protein 2 mitochondrial, A0A1D6P0B5 RING-type E3 ubiquitin transferase, and A0A1D6EI24 ERAD-associated E3 ubiquitin ligase HRD1A (Fig. 1b, Table 1 and S2b).

#### 3.2.1. Protein synthesis and degradation

40S ribosomal protein S4–3 had about a 2-fold decrease in Ni against control ( $P = 0.0506$ ). Combined treatment returned the values to the level of control. Emerging data suggests that constituents of ribosomes can fluctuate, adapting to stresses (Salih et al., 2020). The role of particular subunits during stress is not completely clear. However, some studies speculate on selective translation during various treatments, and our findings support this hypothesis (Fakih et al., 2023; Ramos et al., 2020). The abundance of RING-type E3 ubiquitin transferase (ligase) was about 2 times lower in Ni ( $P = 0.0333$ ) and Ni+Si ( $P = 0.0143$ ) samples than in control—supplement of Si did not alter its level. RING E3 ubiquitin transferase is a crucial enzyme of ubiquitination machinery that participates in root development (Shu and Yang, 2017). During abiotic stresses, its accumulation may be controlled through abscisic acid, ethylene, or mitogen-activated protein kinase (MAPK) signaling pathways (Han et al., 2022). Overexpression of specific RING E3 ligases induced aluminum and cadmium tolerance by indirectly decreasing a heavy metal amount in shoots and roots (Ahmed et al., 2021; Qin et al., 2017). ERAD-associated E3 ubiquitin ligase HRD1A abundance declined 3.8 times under Ni treatment ( $P = 0.0002$ ) and 2.7 times under Ni+Si treatment against control ( $P = 0.0012$ ). Endoplasmic reticulum-associated degradation (ERAD) is a mechanism to control misfolded proteins via proteasome-mediated degradation, whereas E3 guides client proteins to the machinery. It is required for normal plant growth and development and for adapting to environmental stresses (Liu et al., 2021). Researchers showed that in Arabidopsis, HRD1 negatively regulated heat tolerance and accumulation of cuticular lipids (Li et al., 2017; Wu et al., 2021). Thus, a lower abundance of 2 E3 ubiquitin ligases in maize roots in our study may indicate that Ni-treated plants were sensitive to the exposure and Si only partially alleviated such harmful effect.

#### 3.2.2. Lipid metabolism

3-ketoacyl reductase GL8B declined 2 times in Ni-treated samples ( $P = 0.0358$ ), and Si supplement reversed accumulation to the level in control. This protein is a part of fatty acid elongase required for the biosynthesis of very long-chain fatty acids (Dietrich et al., 2005). Our data indicate that Ni stress impacts fatty acid biosynthesis in maize roots, while Si alleviates this effect. Mitochondrial

3-hydroxyisobutyryl-CoA hydrolase-like protein 2 abundance decreased 5 times in Ni-treated samples ( $P = 0.002$ ). Combined treatment (Ni+Si) balanced its level—only 2.2 times lower than control ( $P = 0.0992$ ). This protein is involved in the catabolism of branched-chain amino acids (particularly valine and isoleucine), and its overexpression may lead to their enhanced degradation and higher triacylglycerol content (Pan et al., 2017). Apparently, this process is inhibited in young maize roots.

#### 3.2.3. Nuclear export

The abundance of EXPORTIN 1 A was considerably reduced in Ni samples, while the effect size was less pronounced in combined treatment—3.7- and 2-fold decline compared to control, respectively ( $P = 0.0086$  and  $P = 0.284$ ). This protein maintains protein export from the nucleus (Haasen et al., 1999). Overexpression of rice EXPORTIN 1 led to impaired development but improved salt and drought tolerance compared to a wild type (Peng et al., 2023). Another study showed that EXPORTIN 1A directly interacts with histone deacetylase HDA6 in Arabidopsis (*Arabidopsis thaliana*), thus contributing to epigenetic regulation (Zhu et al., 2019). The role of EXPORTIN 1A in Ni-induced stress in maize roots remains enigmatic.

### 3.3. Functional implications of proteins induced by nickel and less abundant in combined treatment

The smallest cluster 'Ni high, Si low' contained: A0A1D6DVH5 LOX, Q6VB92  $\beta$ -glucanase, B6SYU7 and A0A1D6KZK4 Cox19-like CHCH family proteins, A0A1D6GVS9 MAPK, and A0A1D6EZ64 polygalacturonase inhibitor 1. These six proteins were less abundant in combined treatment than in metal application (Fig. 1b), and the fold change varied from 1.7 to 2.0 (Table 1 and S2b).

#### 3.3.1. Signal transduction

Lipoxygenase was 1.8-fold more abundant in Ni samples ( $P = 0.0755$ ), while in Ni+Si treatment, it declined below the control level. Lipoxygenases (EC 1.13.11.12) oxygenate polyunsaturated fatty acids, typically linoleic and linolenic acids, forming lipid hydroperoxides that, in turn, act as signaling molecules. Lipoxygenase may be a marker of plant stress tolerance (Singh et al., 2022). This enzyme accumulated in wheat organs upon lead treatment (Navabpour et al., 2020). Furthermore, the critical role of LOX activity in root radial expansion was shown under cadmium-induced stress (Alemayehu et al., 2013). The authors also proposed that upregulated LOX activity in barley (*Hordeum vulgare*) roots in the presence of cadmium is a component of stress response rather than responsible for damaging lipid peroxidation (Liptáková et al., 2013). Mitogen-activated protein kinase was 2 times less abundant in Ni+Si samples versus Ni samples ( $P = 0.0043$ ), while the difference between Ni+Si and control was less substantial (1.5-fold decline,  $P = 0.078$ ). It is a part of a signaling cascade where MAPK is phosphorylated and activated by MAPK kinase (MAPKK) and then phosphorylates other substrates (e.g., transcription regulators, other kinases) (Opdenakker et al., 2012). Typically, the level of transcripts of MAPK genes and protein accumulation increases quickly after metal exposure (Agrawal et al., 2002; Majeed et al., 2023). Also, variable activity and protein accumulation patterns were shown in alfalfa (*Medicago sativa*) roots under copper and cadmium exposure: MAPK increased after the treatment started and then decreased (Jonak et al., 2004). Thus, a somewhat lower abundance of both signaling proteins in our combined treatment is logical at the later 9th day of exposure.

#### 3.3.2. Plasmodesmata and cell wall permeability

The abundance of  $\beta$ -glucanase had the same pattern as LOX—1.7-fold increase in samples treated with Ni ( $P = 0.2359$ ) and normalization to control level in Ni+Si.  $\beta$ -1,3-Glucanases regulate the hydrolysis of  $\beta$ -1,3-glucan polymer—callose—thus controlling plasmodesmata permeability, particularly in roots suffering from metal toxicity

(Bardáčová et al., 2016; Piršelová et al., 2012; Sun et al., 2019). Another group showed that heavy metal stress-related  $\beta$ -glucanase decreased callose deposition in response to copper and iron combating inhibition of primary root growth (O'Lexy et al., 2018). Overexpression of  $\beta$ -glucanase in *Arabidopsis* reduced the deposition of aluminium and callose in the roots, increasing tolerance (Zhang et al., 2015). Combined treatment reduced the abundance of polygalacturonase inhibitor 1 about 2 times compared with all other treatments ( $P \leq 0.0335$ ). Interestingly, plant polygalacturonase-inhibiting proteins are described as exclusively extracellular proteins of plant immunity system recognizing and suppressing fungal polygalacturonases, which, in turn, cleave pectin in host cell walls, facilitating infection (Chiu et al., 2021; Kalunke et al., 2015). However, plants, particularly maize, possess their own polygalacturonases, with the described transient expression in pollen (Lu

et al., 2021; Rhee et al., 2003). One study showed that overexpression of a polygalacturonase gene caused higher aluminium deposition in the root elongation zone. Thus, the authors suggested that regulating pectin distribution in the root elongation zone impacts aluminium tolerance (Nagayama et al., 2022). Another study on maize genes bioinformatically screened and identified a polygalacturonase inhibitor gene with root-preferable expression (Li et al., 2019). We provided the first experimental insight into the role of polygalacturonase inhibitors and, indirectly, polygalacturonases in cell wall permeability of roots during Ni stress. Contrasting abundance of  $\beta$ -glucanase and polygalacturonase inhibitor 1 in our data—higher upon Ni exposure yet lower in Ni+Si treatment—might indicate absence of substantial stress in combined experiment.

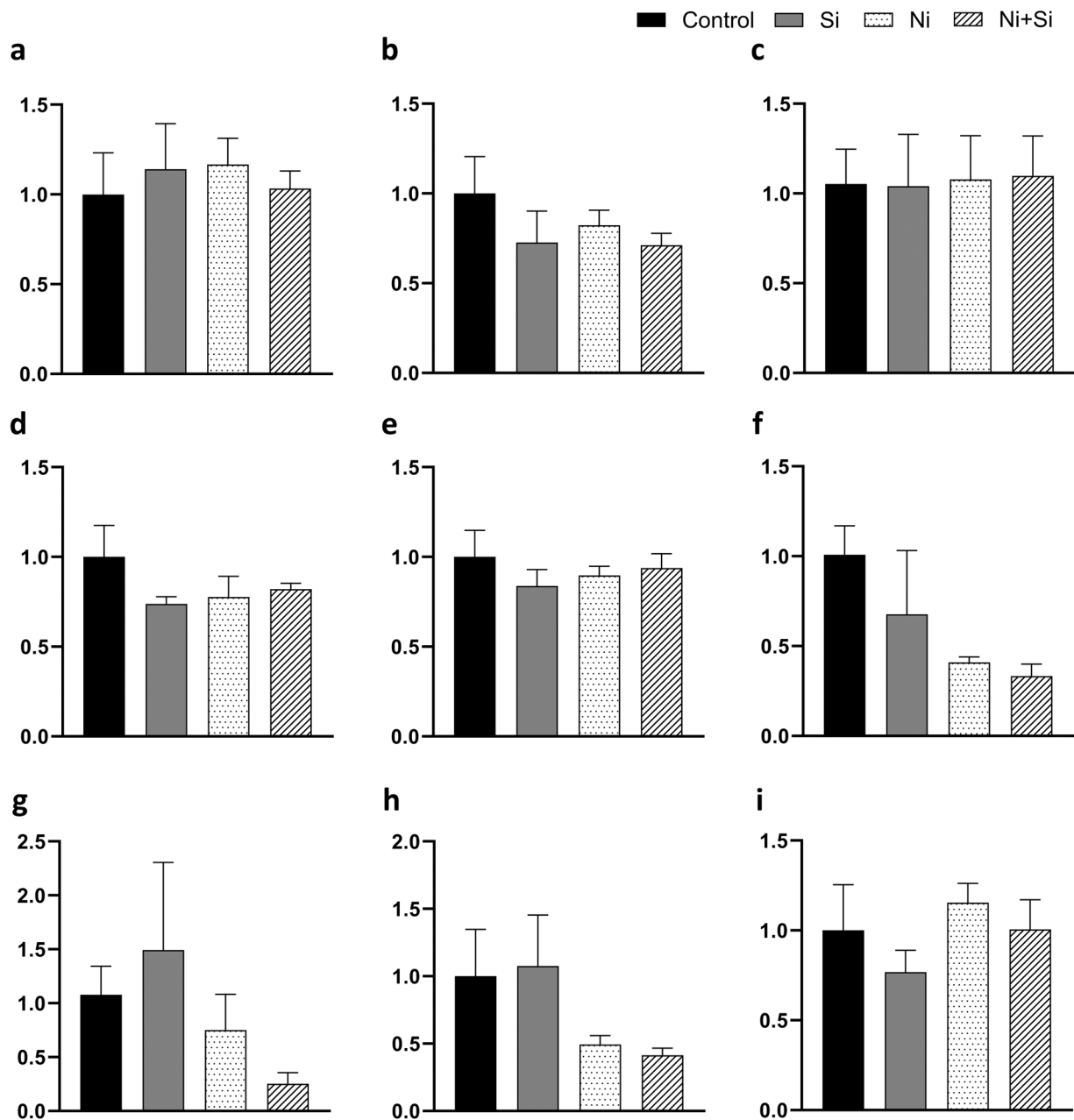


**Fig. 2.** Relative expression of the targeted genes normalized to value in control samples: (a) Lipoxigenase, (b)  $\beta$ -glucanase, (c) mitogen-activated protein kinase, (d) A0A1D6KZK4 Cox19-like CHCH family protein, (e) B6SYU7 Cox19-like CHCH family protein, (f) polygalacturonase inhibitor 1, (g) EC protein homolog, (h) sucrose synthase, and (i) glutathione S-transferase. Roots of 12-day-old maize seedlings were collected after 9 days of treatment. Graphs show means and standard errors of 4 biological replicates. No significant differences were revealed by ANOVA,  $P \leq 0.05$ . Ni refers to 100  $\mu$ M Ni treatment, and Si refers to 2.5 mM Si treatment.

### 3.3.3. Metallochaperones

The accumulation of two Cox19-like CHCH family proteins, B6SYU7 and A0A1D6KZK4, showed a similar pattern—1.7-fold lower abundance in combined treatment ( $P = 0.0146$  and  $P = 0.0273$ , respectively) compared with Ni. Cytochrome c oxidase (COX, EC 7.1.1.9) is the last electron acceptor that controls respiration, contributing to redox and lipid homeostasis. Furthermore, COX includes different modules (Mansilla et al., 2018). Particularly, COX19 is an assembly factor responsible for the insertion of copper. Arabidopsis roots with suppressed COX19 serving as metallochaperone were sensitive to copper and iron (Garcia et al., 2019). The study of Arabidopsis COX genes revealed 2 of them, *AtCOX19-1* and *AtCOX19-2*, encoding COX19 protein, and *AtCOX19-1* expression was triggered by the copper, zinc, and iron treatment (Attallah et al., 2007b). Other reports from these groups supported a hypothesis about the essential role of COX19 metallochaperones under excessive metal toxicity, particularly in roots (Attallah et al., 2007a; Garcia et al., 2016). Our data indicates that COX19-like proteins are not critical for Si-enhanced Ni tolerance at the later exposure phase in maize roots.

### 3.4. Relative gene expression indicated that protein abundance was not transcriptionally regulated

Based on proteomic profiling (Fig. S2), 9 genes were selected for measuring relative expression patterns—6 from the cluster ‘Ni high, Si low’ (LOX,  $\beta$ -glucanase, 2 Cox19-like CHCH family proteins, MAPK, and polygalacturonase inhibitor 1), 2 based on substantial change in effect size across experimental conditions (SuSy and EC protein homolog or metallothionein), and GST showing abundance pattern similar to the last 2 (Fig. 2). Estimation of relative expression after 9 days of exposure failed to detect significant changes among root samples, contrasting proteomic data. The most notable change was observed in the expression pattern of polygalacturonase inhibitor 1, SuSy, and EC protein homolog. Specifically, Ni-treated samples (Ni alone and combined with Si) had a decline of polygalacturonase inhibitor 1 (Fig. 2f) expression 2.7 ( $P = 0.1991$ ) and 3.0 times ( $P = 0.1296$ ), respectively, in comparison with control, largely concordant with protein abundance. Relative expression of EC metallothionein decreased 3.9 times in combined treatment ( $P = 0.6008$ ) against control and 5.5 times versus Si ( $P = 0.2788$ ) (Fig. 2g), almost opposite to protein accumulation data. In Ni+Si treated roots, SuSy expression was 2.4 times lower than in control ( $P = 0.4174$ ) and 2.6 times decreased against Si ( $P = 0.3200$ ) (Fig. 2h). Similar proportion was characteristic for Ni treatment, largely discordant with protein abundance. Of note, comparable MAPK transcription levels among the

samples (Fig. 2c) after 9 days of Ni exposure align with the previous observation during copper and cadmium stress. Researchers reported its quick induction yet returning to control levels during longer exposure (Agrawal et al., 2002; Jonak et al., 2004). Similarly, cadmium-treated roots showed elevated transcription of cytosolic LOX1 after 24 h of treatment (Smeets et al., 2008). Such a low correspondence between mRNA expression level and protein abundance may be explained by different half-lives of mRNA and proteins (Haider and Pal, 2013).

### 3.5. Corn roots showed modified glutathione S-transferase activity

Proteomic profiling revealed a statistically significant 1.5-fold accumulation of GST in samples treated both with Ni and Si compared to control. Then, targeted measurement confirmed a considerable 1.9-fold ( $P = 0.0483$ ) boost of GST activity in Ni+Si samples versus non-treated ones (Fig. 3a). Of note, the expression level of the coding gene remained largely stable.

The activity of LOX (similar to gene expression data) did not reflect the protein abundance alteration in exposed samples against control (Fig. 3b). Conversely, the study on eggplant (*Solanum melongena*) showed elevated activity of LOX in Ni-stressed leaves and confirmed the mitigating effect of NO by a slight reduction of enzymatic activity (Soliman et al., 2019). Another work showed an increase of LOX activity in tomato (*Solanum lycopersicum*) during Ni treatment and a slight protective effect upon applying endophytic bacteria (Badawy et al., 2022).

### 3.6. Silicon application somewhat reduced nickel-induced accumulation of soluble sugars

Remarkable accumulation of SuSy in Ni and Ni+Si treated samples motivated testing content of soluble sugars. Overall, samples with Ni (metal alone and combined treatment) showed higher fructose, glucose, and sucrose content. Specifically, fructose content increased 7.6 times ( $P = 0.0138$ ) in Ni and 5.6 times ( $P = 0.0919$ ) in Ni+Si against control (Fig. 4a). Glucose accumulated in samples with Ni—3.9 times ( $P = 0.0004$ ) and Ni+Si—3.5 times ( $P = 0.0014$ ) compared to control (Fig. 4b). The increase in sucrose content was even more substantial—12-fold in Ni ( $P = 0.0689$ ) and 10-fold in Ni+Si ( $P = 0.1566$ ) versus control (Fig. 4c). While Si alone caused no change in the content of all measured sugars. Apparently, the transport of sucrose to roots increased to fulfill energy needs, and reversible cleavage of sucrose dominated (Stein and Granot, 2019). Conversely, cadmium treatment caused no change in fructose, glucose, and sucrose content in 18-day-old maize roots (C. Li et al., 2020). While in a follow-up study exploring the

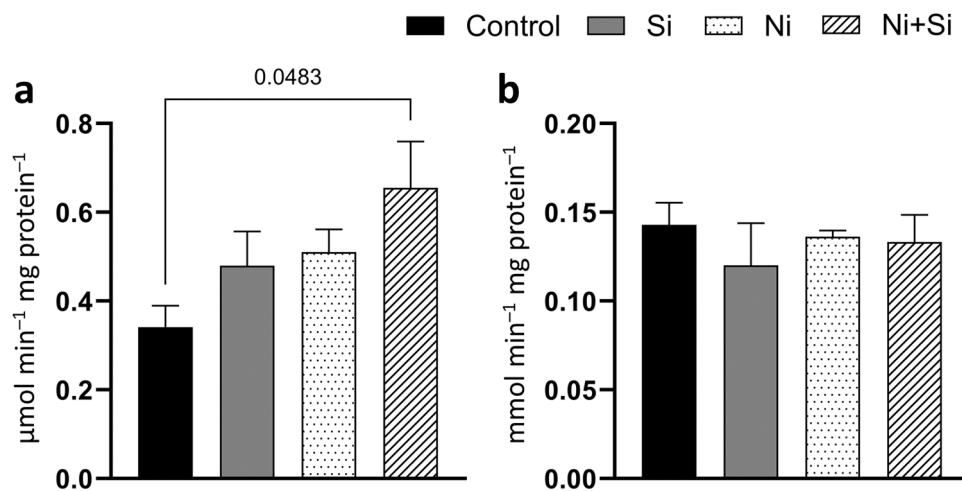


**Fig. 3.** Enzymatic activity assays: (a) Glutathione S-transferase and (b) lipoxigenase. Roots of 12-day-old maize seedlings were collected after 9 days of treatment. Graphs show means and standard errors of 4 biological replicates. Data were evaluated by ANOVA followed by Tukey's test.  $P$ -values for significant pairs are depicted. Ni refers to 100  $\mu\text{M}$  Ni treatment, and Si refers to 2.5 mM Si treatment.



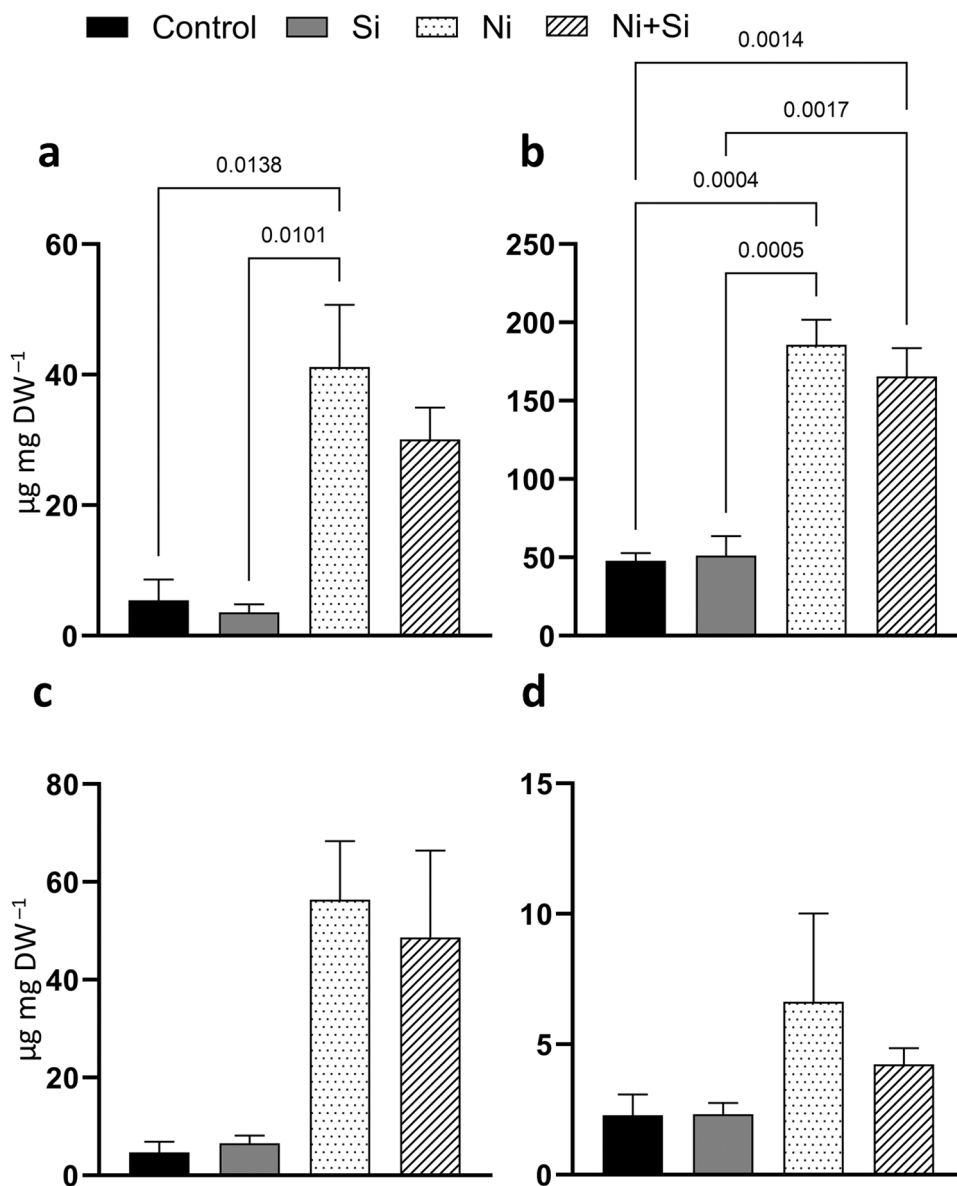


**Fig. 4.** Content of soluble sugars: (a) Fructose, (b) glucose, (c) sucrose, and (d) *myo*-inositol. Roots of 12-day-old maize seedlings were collected after 9 days of treatment. Graphs show means and standard errors of 4 biological replicates. Data were evaluated by ANOVA followed by Tukey's test. *P*-values for significant pairs are depicted. Ni refers to 100  $\mu\text{M}$  Ni treatment, and Si refers to 2.5 mM Si treatment. DW is dry weight.

dynamics of soluble sugars accumulation, the authors showed a lower magnitude of changes in tolerant hybrid, contrasting remarkably increased levels of total sugars, sucrose, fructose, and glucose on the 9th day in the roots of sensitive one (C. Li et al., 2022). The concentration of total sugars in soybean (*Glycine max*) roots progressively declined upon application of higher concentrations of copper, chromium, and Ni (Duan et al., 2020).

We detected a non-significant 2.9-fold increase of *myo*-inositol level upon applying Ni versus control ( $P = 0.4804$ ) (Fig. 4d), whereas, in combined treatment, sugar content was only slightly higher than control. *Myo*-inositol is a product of a glucose-6-phosphate conversion and a substrate for cell wall pectin biosynthesis (Loewus and Murthy, 2000). Recent reports indicated its role in response to abiotic stresses (Hu et al., 2020). Foliar application of *myo*-inositol alleviated salt stress in quinoa (*Chenopodium quinoa*), reducing ROS content, inducing antioxidant enzyme activities, and improving membrane stability (Al-Mushhin et al., 2021). The tolerant lentil (*Vicia lens*) cultivar accumulated *myo*-inositol under drought treatment, whereas the susceptible genotype showed the opposite trend (Foti et al., 2021). *Myo*-inositol-1-phosphate synthase

(catalyzing dephosphorylation of *myo*-inositol-1-phosphate to *myo*-inositol) from golden rain tree (*Koeleruteria paniculata*) contributed to cadmium tolerance. Overexpressing plants accumulated pectin, captured more toxic metal in root cell walls, and decreased its transport to aboveground parts (Zhou et al., 2024). Overall, our data showed that metal, mineral, or combined exposure did not induce substantial detrimental biochemical changes in maize roots, contrasting the remarkable inhibition of root length in Ni and Ni+Si conditions (Fiala et al., 2021).

#### 4. Conclusions

Comprehensive proteomic analysis of root tips suggested plausible mechanisms of Si mitigation effect during Ni toxicity: Chelation by metallothioneins, detoxification by glycine betaine, and restructuring of plasma membrane transporters. A lower abundance of 2 E3 ubiquitin ligases and 40S ribosomal protein in young maize roots could indicate that Ni affects protein synthesis and degradation and Si only partially alleviates toxicity of excessive metal. The role of glutathione-S-transferase detoxification, plausibly through phytochelatin, in

combined treatment was further confirmed by enzymatic activity assay. Reactive accumulation of sucrose synthase and corresponding soluble sugars in Ni and combined treatment suggests high energy requirement under both metal stress and its mitigation. Of note, relative gene expression data of selected coding genes showed marginal concordance with proteomic data, indicating posttranscriptional regulation. We opened avenues for follow-up studies on functional validation of the proposed mitigation mechanisms. Such new knowledge is another step toward the scientifically-backed use of Si for protecting crops grown in metal-contaminated soils.

## Funding sources

This study was supported by the EU NextGenerationEU through the Recovery and Resilience Plan for Slovakia project 09I03-03-V01-00005, Slovak Research and Development Agency grant APVV-20-0545, and Slovak Academy of Sciences project VEGA 2/0103/21.

## CRediT authorship contribution statement

**Ivana Fialová:** Writing – review & editing, Investigation, Funding acquisition, Conceptualization. **Olha Lakhneko:** Writing – original draft, Visualization, Methodology, Investigation, Funding acquisition, Formal analysis. **Maksym Danchenko:** Writing – original draft, Visualization, Methodology, Funding acquisition, Formal analysis. **Andrej Kováč:** Writing – review & editing, Data curation. **Mária Kopáčová:** Writing – review & editing, Methodology. **Roderik Fiala:** Writing – review & editing, Investigation, Conceptualization.

## Declaration of Competing Interest

The authors have no relevant financial or non-financial interests to disclose.

## Acknowledgment

We are grateful to Dr Miroslava Luxová for mentoring and consulting.

## Appendix A. Supporting information

Supplementary data associated with this article can be found in the online version at [doi:10.1016/j.ecoenv.2024.117334](https://doi.org/10.1016/j.ecoenv.2024.117334).

## Data availability

Data are available in the main text of the manuscript and its supplementary materials.

## References

- Abbas, S., Basit, F., Tanwir, K., Zhu, X., Hu, J., Guan, Y., Hu, W., Sheteiwy, M.S., Yang, H., El-Keblawy, A., El-Tarabily, K.A., AbuQamar, S.F., Lou, J., 2023. Exogenously applied sodium nitroprusside alleviates nickel toxicity in maize by regulating antioxidant activities and defense-related gene expression. *Physiol. Plant.* 175, e13985. <https://doi.org/10.1111/pp1.13985>.
- Adrees, M., Ali, S., Rizwan, M., Zia-ur-Rehman, M., Ibrahim, M., Abbas, F., Farid, M., Qayyum, M.F., Irshad, M.K., 2015. Mechanisms of silicon-mediated alleviation of heavy metal toxicity in plants: A review. *Ecotoxicol. Environ. Saf.* 119, 186–197. <https://doi.org/10.1016/j.ecoenv.2015.05.011>.
- Agrawal, G.K., Rakwal, R., Iwahashi, H., 2002. Isolation of novel rice (*Oryza sativa* L.) multiple stress responsive MAP kinase gene, *OsMSRMK2*, whose mRNA accumulates rapidly in response to environmental cues. *Biochem. Biophys. Res. Commun.* 294, 1009–1016. [https://doi.org/10.1016/S0006-291X\(02\)00571-5](https://doi.org/10.1016/S0006-291X(02)00571-5).
- Ahammed, G.J., Li, C.-X., Li, X., Liu, A., Chen, S., Zhou, J., 2021. Overexpression of tomato RING E3 ubiquitin ligase gene *SIRING1* confers cadmium tolerance by attenuating cadmium accumulation and oxidative stress. *Physiol. Plant.* 173, 449–459. <https://doi.org/10.1111/pp1.13294>.
- Alemayehu, A., Bočová, B., Zelinová, V., Mistrík, I., Tamás, L., 2013. Enhanced lipoxygenase activity is involved in barley root tip swelling induced by cadmium, auxin or hydrogen peroxide. *Environ. Exp. Bot.* 93, 55–62. <https://doi.org/10.1016/j.envexpbot.2013.06.004>.
- Al-Mushhin, A.A.M., Qari, S.H., Fakhr, M.A., Alnusairi, G.S.H., Alnusaire, T.S., AlRashidi, A.A., Latef, A.A., Ali, O.M., Khan, A.A., Soliman, M.H., 2021. Exogenous myo-inositol alleviates salt stress by enhancing antioxidants and membrane stability via the upregulation of stress responsive genes in *Chenopodium quinoa* L. *Plants* 10, 2416. <https://doi.org/10.3390/plants10112416>.
- Amjad, M., Raza, H., Murtaza, B., Abbas, G., Imran, M., Shahid, M., Naeem, M.A., Zakir, A., Iqbal, M.M., 2020. Nickel toxicity induced changes in nutrient dynamics and antioxidant profiling in two maize (*Zea mays* L.) hybrids. *Plants* 9. <https://doi.org/10.3390/plants9010005>.
- Attallah, C.V., Welchen, E., Gonzalez, D.H., 2007a. The promoters of *Arabidopsis thaliana* genes *AtCOX17-1* and *-2*, encoding a copper chaperone involved in cytochrome c oxidase biogenesis, are preferentially active in roots and anthers and induced by biotic and abiotic stress. *Physiol. Plant.* 129, 123–134. <https://doi.org/10.1111/j.1399-3054.2006.00776.x>.
- Attallah, C.V., Welchen, E., Pujol, C., Bonnard, G., Gonzalez, D.H., 2007b. Characterization of *Arabidopsis thaliana* genes encoding functional homologues of the yeast metal chaperone Cox19p, involved in cytochrome c oxidase biogenesis. *Plant Mol. Biol.* 65, 343–355. <https://doi.org/10.1007/s11103-007-9224-1>.
- Badawy, I.H., Hmed, A.A., Sofy, M.R., Al-Mokadem, A.Z., 2022. Alleviation of cadmium and nickel toxicity and phyto-stimulation of tomato plant L. by endophytic *Micrococcus luteus* and *Enterobacter cloacae*. *Plants* 11, 2018. <https://doi.org/10.3390/plants11152018>.
- Bardáčová, M., Maglovski, M., Gregorová, Z., Konotop, Y., Horník, M., Moravčíková, J., Kraic, J., Mihálik, D., Matusiková, I., 2016. The activity of cell-wall modifying  $\beta$ -1,3-glucanases in soybean grown in presence of heavy metals. *Nova Biotechnol. Et. Chim.* 15, 114–121. <https://doi.org/10.1515/nbec-2016-0012>.
- Butt, H., Bazin, J., Prasad, K.V.S.K., Awad, N., Crespi, M., Reddy, A.S.N., Mahfouz, M.M., 2022. The rice serine/arginine splicing factor RS33 regulates pre-mRNA splicing during abiotic stress responses. *Cells* 11, 1796. <https://doi.org/10.3390/cells11111796>.
- Chiu, T., Behari, A., Chartron, J.W., Putman, A., Li, Y., 2021. Exploring the potential of engineering polygalacturonase-inhibiting protein as an ecological, friendly, and nontoxic pest control agent. *Biotechnol. Bioeng.* 118, 3200–3214. <https://doi.org/10.1002/bit.27845>.
- Choudhury, B., Mitra, S., Biswas, A.K., 2010. Regulation of sugar metabolism in rice (*Oryza sativa* L.) seedlings under arsenate toxicity and its improvement by phosphate. *Physiol. Mol. Biol. Plants* 16, 59–68. <https://doi.org/10.1007/s12298-010-0008-8>.
- Chronopoulou, E., Kontouri, K., Chantzikonstantinou, M., Poulou, F., Perperopoulou, F., Voulgari, G., Bosmalis, E., Axarli, I., Nianiou-Obeidat, I., Madesis, P., 2014. Plant glutathione transferases: structure, antioxidant catalytic function and in planta protective role in biotic and abiotic stress. *Curr. Chem. Biol.* 8, 58–75. <https://doi.org/10.2174/2212796809666150302213733>.
- Cocker, K.M., Evans, D.E., Hodson, M.J., 1998. The amelioration of aluminium toxicity by silicon in higher plants: Solution chemistry or an in planta mechanism? *Physiol. Plant.* 104, 608–614. <https://doi.org/10.1034/j.1399-3054.1998.1040413.x>.
- Cooke, J., Leishman, M.R., 2011. Is plant ecology more siliceous than we realise? *Trends Plant Sci.* 16, 61–68. <https://doi.org/10.1016/j.tplants.2010.10.003>.
- Czékus, Z., Farkas, M., Bakacsy, L., Ördög, A., Gallé, Á., Poór, P., 2020. Time-dependent effects of bentazon application on the key antioxidant enzymes of soybean and common ragweed. *Sustainability* 12, 3872. <https://doi.org/10.3390/su12093872>.
- van der Voet, E., Salminen, R., Eckelman, M., Mudd, G., Norgate, T., Norgate, R., 2013. Environmental risks and challenges of anthropogenic metals flows and cycles, A report of the working group on the global metal flows to the international resource panel. UNEP.
- Deshmukh, R.K., Vivancos, J., Guérin, V., Sonah, H., Labbé, C., Belzile, F., Bélanger, R.R., 2013. Identification and functional characterization of silicon transporters in soybean using comparative genomics of major intrinsic proteins in *Arabidopsis* and rice. *Plant Mol. Biol.* 83, 303–315. <https://doi.org/10.1007/s11103-013-0087-3>.
- Deshmukh, R.K., Vivancos, J., Ramakrishnan, G., Guérin, V., Carpentier, G., Sonah, H., Labbé, C., Isenring, P., Belzile, F.J., Bélanger, R.R., 2015. A precise spacing between the NPA domains of aquaporins is essential for silicon permeability in plants. *Plant J.* 83, 489–500. <https://doi.org/10.1111/tpj.12904>.
- Devi, R., Munjal, N., Gupta, A.K., Kaur, N., 2007. Cadmium induced changes in carbohydrate status and enzymes of carbohydrate metabolism, glycolysis and pentose phosphate pathway in pea. *Environ. Exp. Bot.* 61, 167–174. <https://doi.org/10.1016/j.envexpbot.2007.05.006>.
- Dietrich, C.R., Perera, M.A.D.N., D. Yandeau-Nelson, M., Meeley, R.B., Nikolau, B.J., Schnable, P.S., 2005. Characterization of two GL8 paralogs reveals that the 3-ketoacyl reductase component of fatty acid elongase is essential for maize (*Zea mays* L.) development. *Plant J.* 42, 844–861. <https://doi.org/10.1111/j.1365-3113.2005.02418.x>.
- Dinakar, N., Nagaiyothi, P., Suresh, S., Thoti, Challa, S., 2009. Cadmium induced changes on proline, antioxidant enzymes, nitrate and nitrite reductases in *Arachis hypogaea* L. *J. Environ. Biol. / Acad. Environ. Biol.*, India 30, 289–294.
- Distler, U., Kuharev, J., Navarro Álvarez, P., Tenzer, S., 2016. Label-free quantification in ion mobility-enhanced data-independent acquisition proteomics. *Nat. Protoc.* 11, 795–812. <https://doi.org/10.1038/nprot.2016.042>.
- Dixit, P., Mukherjee, P.K., Ramachandran, V., Eapen, S., 2011. Glutathione transferase from *Trichoderma virens* enhances cadmium tolerance without enhancing its accumulation in transgenic *Nicotiana tabacum*. *PLOS ONE* 6, e16360. <https://doi.org/10.1371/journal.pone.0016360>.

- Dixon, N.E., Gazzola, C., Blakeley, R.L., Zerner, B., 1975. Jack bean urease (EC 3.5.1.5). Metalloenzyme. Simple biological role for nickel. *J. Am. Chem. Soc.* 97, 4131–4133. <https://doi.org/10.1021/ja00847a045>.
- Duan, Y., Sangani, C., Muddassir, M., Soni, K., 2020. Copper, chromium and nickel heavy metal effects on total sugar and protein content in *Glycine max*. Research Square. <https://doi.org/10.21203/rs.3.rs-107829/v1>.
- El-Naggar, A., Ahmed, N., Mosa, A., Niaz, N.K., Yousaf, B., Sharma, A., Sarkar, B., Cai, Y., Chang, S.X., 2021. Nickel in soil and water: Sources, biogeochemistry, and remediation using biochar. *J. Hazard. Mater.* 419, 126421. <https://doi.org/10.1016/j.jhazmat.2021.126421>.
- Erenstein, O., Jaleta, M., Sonder, K., Mottaleb, K., Prasanna, B.M., 2022. Global maize production, consumption and trade: trends and R&D implications. *Food Secur.* 14, 1295–1319. <https://doi.org/10.1007/s12571-022-01288-7>.
- Fakih, Z., Plourde, M.B., Germain, H., 2023. Differential participation of plant ribosomal proteins from the small ribosomal subunit in protein translation under stress. *Biomolecules* 13, 1160. <https://doi.org/10.3390/biom13071160>.
- FAO, 2022. Food Outlook – Biannual Report on Global Food Markets, Food Outlook. FAO, Rome.
- Feng, T., He, X., Zhuo, R., Qiao, G., Han, X., Qiu, W., Chi, L., Zhang, D., Liu, M., 2020. Identification and functional characterization of ABC transporters for Cd tolerance and accumulation in *Sedum alfredii* Hance. *Sci. Rep.* 10, 20928. <https://doi.org/10.1038/s41598-020-78018-6>.
- Fiala, R., Fialová, I., Vaculík, M., Luxová, M., 2021. Effect of silicon on the young maize plants exposed to nickel stress. *Plant Physiol. Biochem.* 166, 645–656. <https://doi.org/10.1016/j.plaphy.2021.06.026>.
- Foti, C., Kalampokis, I.F., Aliferis, K.A., Pavli, O.I., 2021. Metabolic responses of two contrasting lentil genotypes to PEG-induced drought stress. *Agronomy* 11, 1190. <https://doi.org/10.3390/agronomy11061190>.
- Fu, S., Lu, Y., Zhang, X., Yang, G., Chao, D., Wang, Z., Shi, M., Chen, J., Chao, D.-Y., Li, R., Ma, J.F., Xia, J., 2019. The ABC transporter ABCG36 is required for cadmium tolerance in rice. *J. Exp. Bot.* 70, 5909–5918. <https://doi.org/10.1093/jxb/erz335>.
- Gao, C., Zhuang, X., Shen, J., Jiang, L., 2017. Plant ESCRT complexes: Moving beyond endosomal sorting. *Trends Plant Sci.* 22, 986–998. <https://doi.org/10.1016/j.tplants.2017.08.003>.
- Garcia, L., Welchen, E., Gey, U., Arce, A.L., Steinebrunner, I., Gonzalez, D.H., 2016. The cytochrome c oxidase biogenesis factor ATCOX17 modulates stress responses in *Arabidopsis*. *Plant. Cell Environ.* 39, 628–644. <https://doi.org/10.1111/pce.12647>.
- Garcia, L., Mansilla, N., Ocampos, N., Pagani, M.A., Welchen, E., Gonzalez, D.H., 2019. The mitochondrial copper chaperone COX19 influences copper and iron homeostasis in *Arabidopsis*. *Plant Mol. Biol.* 99, 621–638. <https://doi.org/10.1007/s11103-019-00840-y>.
- Gerendás, J., Polacco, J.C., Freyermuth, S.K., Sattelmacher, B., 1999. Significance of nickel for plant growth and metabolism. *J. Plant Nutr.* 162, 241–256. [https://doi.org/10.1002/\(SICI\)1522-2624\(199906\)162:3<241::AID-JPLN241>3.0.CO;2-Q](https://doi.org/10.1002/(SICI)1522-2624(199906)162:3<241::AID-JPLN241>3.0.CO;2-Q).
- Ghosh, S., Saha, J., Biswas, A.K., 2013. Interactive influence of arsenate and selenate on growth and nitrogen metabolism in wheat (*Triticum aestivum* L.) seedlings. *Acta Physiol. Plant.* 35, 1873–1885. <https://doi.org/10.1007/s11738-013-1225-x>.
- Głowacka, K., Żróbek-Sokolnik, A., Okorski, A., Najdzion, J., 2019. The effect of cadmium on the activity of stress-related enzymes and the ultrastructure of pea roots. *Plants* 8, 413. <https://doi.org/10.3390/plants8100413>.
- Gu, H.-H., Qiu, H., Tian, T., Zhan, S.-S., Deng, T.-H.-B., Chaney, R.L., Wang, S.-Z., Tang, Y.-T., Morel, J.-L., Qiu, R.-L., 2011. Mitigation effects of silicon rich amendments on heavy metal accumulation in rice (*Oryza sativa* L.) planted on multi-metal contaminated acidic soil. *Chemosphere* 83, 1234–1240. <https://doi.org/10.1016/j.chemosphere.2011.03.014>.
- Haasen, D., Köhler, C., Neuhaus, G., Merkle, T., 1999. Nuclear export of proteins in plants: AtXPO1 is the export receptor for leucine-rich nuclear export signals in *Arabidopsis thaliana*. *Plant J.* 20, 695–705. <https://doi.org/10.1046/j.1365-3113.1999.00644.x>.
- Haider, S., Pal, R., 2013. Integrated analysis of transcriptomic and proteomic data. *Curr. Genom.* 14, 91–110. <https://doi.org/10.2174/1389202911314020003>.
- Han, G., Qiao, Z., Li, Y., Yang, Z., Wang, C., Zhang, Y., Liu, L., Wang, B., 2022. RING zinc finger proteins in plant abiotic stress tolerance. *Front. Plant Sci.* 13, 877011. <https://doi.org/10.3389/fpls.2022.877011>.
- He, X., Feng, T., Zhang, D., Zhuo, R., Liu, M., 2019. Identification and comprehensive analysis of the characteristics and roles of leucine-rich repeat receptor-like protein kinase (LRR-RLK) genes in *Sedum alfredii* Hance responding to cadmium stress. *Ecotoxicol. Environ. Saf.* 167, 95–106. <https://doi.org/10.1016/j.ecoenv.2018.09.122>.
- Hu, L., Zhou, K., Ren, G., Yang, S., Liu, Y., Zhang, Z., Li, Y., Gong, X., Ma, F., 2020. Myo-inositol mediates reactive oxygen species-induced programmed cell death via salicylic acid-dependent and ethylene-dependent pathways in apple. *Hortic. Res.* 7, 138. <https://doi.org/10.1038/s41438-020-00357-2>.
- Isaacson, T., Damasceno, C.M.B., Saravanan, R.S., He, Y., Catalá, C., Saladié, M., Rose, J. K.C., 2006. Sample extraction techniques for enhanced proteomic analysis of plant tissues. *Nat. Protoc.* 1, 769–774. <https://doi.org/10.1038/nprot.2006.102>.
- Jonak, C., Nakagami, H., Hirt, H., 2004. Heavy metal stress. Activation of distinct mitogen-activated protein kinase pathways by copper and cadmium. *Plant Physiol.* 136, 3276–3283. <https://doi.org/10.1104/pp.104.045724>.
- Kalunke, R.M., Tundo, S., Benedetti, M., Cervone, F., De Lorenzo, G., D'Ovidio, R., 2015. An update on polygalacturonase-inhibiting protein (PGIP), a leucine-rich repeat protein that protects crop plants against pathogens. *Front. Plant Sci.* 6, 146. <https://doi.org/10.3389/fpls.2015.00146>.
- Kim, Y.-H., Khan, A.L., Kim, D.-H., Lee, S.-Y., Kim, K.-M., Waqas, M., Jung, H.-Y., Shin, J.-H., Kim, J.-G., Lee, I.-J., 2014. Silicon mitigates heavy metal stress by regulating P-type heavy metal ATPases, *Oryza sativa* low silicon genes, and endogenous phytohormones. *BMC Plant Biol.* 14, 13. <https://doi.org/10.1186/1471-2229-14-13>.
- Konieczna, W., Mierek-Adamska, A., Chojnacka, N., Antoszewski, M., Szydłowska-Czeriak, A., Dąbrowska, G.B., 2023. Characterization of the metallothionein gene family in *Avena sativa* L. and the gene expression during seed germination and heavy metal stress. *Antioxidants* 12, 1865. <https://doi.org/10.3390/antiox12101865>.
- Laloum, T., Martin, G., Duque, P., 2018. Alternative splicing control of abiotic stress responses. *Trends Plant Sci.* 23, 140–150. <https://doi.org/10.1016/j.tplants.2017.09.019>.
- Li, C., Liu, Y., Tian, J., Zhu, Y., Fan, J., 2020. Changes in sucrose metabolism in maize varieties with different cadmium sensitivities under cadmium stress. *PLOS ONE* 15, e0243835. <https://doi.org/10.1371/journal.pone.0243835>.
- Li, C., Cao, Y., Li, T., Guo, M., Ma, X., Zhu, Y., Fan, J., 2022. Changes in antioxidant system and sucrose metabolism in maize varieties exposed to Cd. *Environ. Sci. Pollut. Res.* 29, 64999–65011. <https://doi.org/10.1007/s11356-022-20422-8>.
- Li, L.-M., Lü, S.-Y., Li, R.-J., 2017. The *Arabidopsis* endoplasmic reticulum associated degradation pathways are involved in the regulation of heat stress response. *Biochem. Biophys. Res. Commun.* 487, 362–367. <https://doi.org/10.1016/j.bbrc.2017.04.066>.
- Li, Y., Liu, X., Chen, R., Tian, J., Fan, Y., Zhou, X., 2019. Genome-scale mining of root-preferential genes from maize and characterization of their promoter activity. *BMC Plant Biol.* 19, 584. <https://doi.org/10.1186/s12870-019-2198-8>.
- Lim, J.D., Hahn, S.J., Yu, C.Y., Chung, I.M., 2005. Expression of the glutathione S-transferase gene (NT107) in transgenic *Dianthus superbus*. *Plant Cell, Tissue Organ Cult.* 80, 277–286. <https://doi.org/10.1007/s11240-004-1032-6>.
- Lin, C.-Y., Trinh, N.N., Fu, S.-F., Hsiung, Y.-C., Chia, L.-C., Lin, C.-W., Huang, H.-J., 2013. Comparison of early transcriptome responses to copper and cadmium in rice roots. *Plant Mol. Biol.* 81, 507–522. <https://doi.org/10.1007/s11103-013-0020-9>.
- Lin, Y., Zhang, C., Lan, H., Gao, S., Liu, H., Liu, J., Cao, M., Pan, G., Rong, T., Zhang, S., 2014. Validation of potential reference genes for qPCR in maize across abiotic stresses, hormone treatments, and tissue types. *PLOS ONE* 9, e95445. <https://doi.org/10.1371/journal.pone.0095445>.
- Ling, Y., Mahfouz, M.M., Zhou, S., 2021. Pre-mRNA alternative splicing as a modulator for heat stress response in plants. *Trends Plant Sci.* 26, 1153–1170. <https://doi.org/10.1016/j.tplants.2021.07.008>.
- Liptáková, L., Huttová, J., Mistrík, I., Tamás, L., 2013. Enhanced lipoxygenase activity is involved in the stress response but not in the harmful lipid peroxidation and cell death of short-term cadmium-treated barley root tip. *J. Plant Physiol.* 170, 646–652. <https://doi.org/10.1016/j.jplph.2012.12.007>.
- Liu, C.-J., 2022. Cytochrome b5: A versatile electron carrier and regulator for plant metabolism. *Front. Plant Sci.* 13, 984174. <https://doi.org/10.3389/fpls.2022.984174>.
- Liu, D., Liu, Y., Rao, J., Wang, G., Li, H., Ge, F., Chen, C., 2013. Overexpression of the glutathione S-transferase gene from *Pyrus pyrifolia* fruit improves tolerance to abiotic stress in transgenic tobacco plants. *Mol. Biol.* 47, 515–523. <https://doi.org/10.1134/S0026893313040109>.
- Liu, R., Xia, R., Xie, Q., Wu, Y., 2021. Endoplasmic reticulum-related E3 ubiquitin ligases: Key regulators of plant growth and stress responses. *Plant Commun.* 2, 100186. <https://doi.org/10.1016/j.xplc.2021.100186>.
- Loewus, F.A., Murthy, P.P.N., 2000. Myo-inositol metabolism in plants. *Plant Sci.* 150, 1–19. [https://doi.org/10.1016/S0168-9452\(99\)00150-8](https://doi.org/10.1016/S0168-9452(99)00150-8).
- Lu, L., Hou, Q., Wang, L., Zhang, T., Zhao, W., Yan, T., Zhao, L., Li, J., Wan, X., 2021. Genome-wide identification and characterization of polygalacturonase gene family in maize (*Zea mays* L.). *Int. J. Mol. Sci.* 22, 10722. <https://doi.org/10.3390/ijms221910722>.
- Majeed, Y., Zhu, X., Zhang, N., ul-Ain, N., Raza, A., Haider, F.U., Si, H., 2023. Harnessing the role of mitogen-activated protein kinases against abiotic stresses in plants. *Front. Plant Sci.* 14, 932923. <https://doi.org/10.3389/fpls.2023.932923>.
- Mansilla, N., Racca, S., Gras, D.E., Gonzalez, D.H., Welchen, E., 2018. The complexity of mitochondrial complex IV: An update of cytochrome c oxidase biogenesis in plants. *Int. J. Mol. Sci.* 19, 662. <https://doi.org/10.3390/ijms19030662>.
- Marengo, R.A., Lopes, N.F., Moreira, M.A., 1995. Photosynthesis and leaf lipoxygenase activity in soybean genotypes lacking seed lipoxygenases isozymes. *Rev. Bras. De. Fisiol. Veg.* 7, 21–25.
- Ministry of the Environment, Finland, 2007. Government decree on the assessment of soil contamination and remediation needs.
- Mir, R.A., Bhat, B.A., Yousuf, H., Islam, S.T., Raza, A., Rizvi, M.A., Charagh, S., Albaqami, M., Sofi, P.A., Zargar, S.A., 2022. Multidimensional role of silicon to activate resilient plant growth and to mitigate abiotic stress. *Front. Plant Sci.* 13, 819658. <https://doi.org/10.3389/fpls.2022.819658>.
- Morón, A., Martín-González, A., Díaz, S., Gutiérrez, J.C., Amaro, F., 2022. Autophagy and lipid droplets are a defense mechanism against toxic copper oxide nanotubes in the eukaryotic microbial model *Tetrahymena thermophila*. *Sci. Total Environ.* 847, 157580. <https://doi.org/10.1016/j.scitotenv.2022.157580>.
- Mosesso, N., Nagel, M.-K., Isono, E., 2019. Ubiquitin recognition in endocytic trafficking – with or without ESCRT-0. *J. Cell Sci.* 132, jcs232868. <https://doi.org/10.1242/jcs.232868>.
- Moulinier-Anzola, J., Schwihla, M., De-Araújo, L., Artner, C., Jörg, L., Konstantinova, N., Luschning, C., Korbei, B., 2020. TOLs function as ubiquitin receptors in the early steps of the ESCRT pathway in higher plants. *Mol. Plant* 13, 717–731. <https://doi.org/10.1016/j.molp.2020.02.012>.
- Mustafa, A., Zulfikar, U., Mumtaz, M.Z., Radziemska, M., Haider, F.U., Holatko, J., Hammersmiedt, T., Naveed, M., Ali, H., Kintl, A., Saeed, Q., Kucerik, J., Brtnicky, M., 2023. Nickel (Ni) phytotoxicity and detoxification mechanisms: A



- review. *Chemosphere* 328, 138574. <https://doi.org/10.1016/j.chemosphere.2023.138574>.
- Naaz, S., Ahmad, N., Jameel, M.R., Al-Huqail, A.A., Khan, F., Qureshi, M.I., 2023. Impact of some toxic metals on important ABC transporters in soybean (*Glycine max* L.). *ACS Omega* 8, 27597–27611. <https://doi.org/10.1021/acsomega.3c03325>.
- Nagayama, T., Tatsumi, A., Nakamura, A., Yamaji, N., Satoh, S., Furukawa, J., Iwai, H., 2022. Effects of polygalacturonase overexpression on pectin distribution in the elongation zones of roots under aluminium stress. *AoB PLANTS* 14, plac003. <https://doi.org/10.1093/aobpla/plac003>.
- Navabpour, S., Yamchi, A., Bagherikia, S., Kafi, H., 2020. Lead-induced oxidative stress and role of antioxidant defense in wheat (*Triticum aestivum* L.). *Physiol. Mol. Biol. Plants* 26, 793–802. <https://doi.org/10.1007/s12298-020-00777-3>.
- O'Leary, R., Kasai, K., Clark, N., Fujiwara, T., Sozzani, R., Gallagher, K.L., 2018. Exposure to heavy metal stress triggers changes in plasmodesmatal permeability via deposition and breakdown of callose. *J. Exp. Bot.* 69, 3715–3728. <https://doi.org/10.1093/jxb/ery171>.
- Olmzahn, J.A., Carvalho, P., 2019. Dynamics and functions of lipid droplets. *Nat. Rev. Mol. Cell Biol.* 20, 137–155. <https://doi.org/10.1038/s41580-018-0085-z>.
- Opdenakker, K., Remans, T., Vangronsveld, J., Cuypers, A., 2012. Mitogen-activated protein (MAP) kinases in plant metal stress: regulation and responses in comparison to other biotic and abiotic stresses. *Int. J. Mol. Sci.* 13, 7828–7853. <https://doi.org/10.3390/ijms13067828>.
- Pan, Y., Yang, J., Gong, Y., Li, X., Hu, H., 2017. 3-Hydroxyisobutyryl-CoA hydrolase involved in isoleucine catabolism regulates triacylglycerol accumulation in *Phaeodactylum tricornutum*. *Philos. Trans. R. Soc. B: Biol. Sci.* 372, 20160409. <https://doi.org/10.1098/rstb.2016.0409>.
- Pan, Y., Zhu, M., Wang, S., Ma, G., Huang, X., Qiao, C., Wang, R., Xu, X., Liang, Y., Lu, K., Li, J., Qu, C., 2018. Genome-wide characterization and analysis of metallothionein family genes that function in metal stress tolerance in *Brassica napus* L. *Int. J. Mol. Sci.* 19, 2181. <https://doi.org/10.3390/ijms19082181>.
- Patankar, H.V., Al-Kharasi, I., Al-Kharasi, L., Jana, G.A., Al-Yahyai, R., Sunkar, R., Yaish, M.W., 2019. Overexpression of a metallothionein 2A gene from date palm confers abiotic stress tolerance to yeast and *Arabidopsis thaliana*. *Int. J. Mol. Sci.* 20. <https://doi.org/10.3390/ijms20122871>.
- Peng, Q., Qiu, J., Li, X., Xu, X., Peng, X., Zhu, G., 2023. The nuclear export receptor OsXPO1 is required for rice development and involved in abiotic stress responses. *Crop J.* 11, 71–78. <https://doi.org/10.1016/j.cj.2022.06.008>.
- Pfaffl, M.W., 2001. A new mathematical model for relative quantification in real-time RT-PCR. *e45–e45 Nucleic Acids Res.* 29. <https://doi.org/10.1093/nar/29.9.e45>.
- Pirselová, H.V., Mistriková, V., Libantová, J., Moravčíková, J., Matušiková, I., 2012. Study on metal-triggered callose deposition in roots of maize and soybean. *Biologia* 67, 698–705. <https://doi.org/10.2478/s11756-012-0051-8>.
- Qin, X., Huang, S., Liu, Y., Bian, M., Shi, W., Zuo, Z., Yang, Z., 2017. Overexpression of A RING finger ubiquitin ligase gene *AtATRF1* enhances aluminium tolerance in *Arabidopsis thaliana*. *J. Plant Biol.* 60, 66–74. <https://doi.org/10.1007/s12374-016-0903-9>.
- Ragsdale, S.W., 2009. Nickel-based enzyme systems. *J. Biol. Chem.* 284, 18571–18575. <https://doi.org/10.1074/jbc.R900020200>.
- Rahman, S., Ahmad, I., Nafees, M., 2023. Mitigation of heavy metal stress in maize (*Zea mays* L.) through application of silicon nanoparticles. *Biocatal. Agric. Biotechnol.* 50, 102757. <https://doi.org/10.1016/j.bcab.2023.102757>.
- Rajakumar, S., Abhishek, A., Selvam, G.S., Nachiappan, V., 2020. Effect of cadmium on essential metals and their impact on lipid metabolism in *Saccharomyces cerevisiae*. *Cell Stress Chaperon* 25, 19–33. <https://doi.org/10.1007/s12192-019-01058-z>.
- Ramos, R.S., Casati, P., Spampinato, C.P., Falcone Ferreyra, M.L., 2020. Ribosomal protein RPL10A contributes to early plant development and abscisic acid-dependent responses in *Arabidopsis*. *Front. Plant Sci.* 11, 582353. <https://doi.org/10.3389/fpls.2020.582353>.
- Ranjana, A., Sinha, R., Bala, M., Pareek, A., Singla-Pareek, S.L., Singh, A.K., 2021. Silicon-mediated abiotic and biotic stress mitigation in plants: Underlying mechanisms and potential for stress resilient agriculture. *Plant Physiol. Biochem.* 163, 15–25. <https://doi.org/10.1016/j.plaphy.2021.03.044>.
- Rhee, S.Y., Osborne, E., Poindexter, P.D., Somerville, C.R., 2003. Microspore separation in the *quartet* 3 mutants of *Arabidopsis* is impaired by a defect in a developmentally regulated polygalacturonase required for pollen mother cell wall degradation. *Plant Physiol.* 133, 1170–1180. <https://doi.org/10.1104/pp.103.028266>.
- Romdhane, L., Panozzo, A., Radhouane, L., Dal Cortivo, C., Barion, G., Vamerali, T., 2021. Root characteristics and metal uptake of maize (*Zea mays* L.) under extreme soil contamination. *Agronomy* 11, 178. <https://doi.org/10.3390/agronomy11010178>.
- Rosenkranz, R.R.E., Bachiri, S., Vraggalas, S., Keller, M., Simm, S., Schleiff, E., Fragkostefanakis, S., 2021. Identification and regulation of tomato serine/arginine-rich proteins under high temperatures. *Front. Plant Sci.* 12, 645689. <https://doi.org/10.3389/fpls.2021.645689>.
- Ruiz-Huerta, E.A., Armenta-Hernández, M.A., Dubrovsky, J.G., Gómez-Bernal, J.M., 2022. Bioaccumulation of heavy metals and As in maize (*Zea mays* L.) grown close to mine tailings strongly impacts plant development. *Ecotoxicology* 31, 447–467. <https://doi.org/10.1007/s10646-022-02522-w>.
- Salih, K.J., Duncan, O., Li, L., O'Leary, B., Fenske, R., Trösch, J., Millar, A.H., 2020. Impact of oxidative stress on the function, abundance, and turnover of the *Arabidopsis* 80S cytosolic ribosome. *Plant J.* 103, 128–139. <https://doi.org/10.1111/tpj.14713>.
- Sanz-Luque, E., Chamizo-Ampudia, A., Llamas, A., Galvan, A., Fernandez, E., 2015. Understanding nitrate assimilation and its regulation in microalgae. *Front. Plant Sci.* 6, 899. <https://doi.org/10.3389/fpls.2015.00899>.
- Shahzad, B., Tanveer, M., Rehman, A., Cheema, S.A., Fahad, S., Rehman, S., Sharma, A., 2018. Nickel; whether toxic or essential for plants and environment - A review. *Plant Physiol. Biochem.* 132, 641–651. <https://doi.org/10.1016/j.plaphy.2018.10.014>.
- Shao, Q., Liu, X., Su, T., Ma, C., Wang, P., 2019. New insights into the role of seed oil body proteins in metabolism and plant development. *Front. Plant Sci.* 10, 1568. <https://doi.org/10.3389/fpls.2019.01568>.
- Sheoran, I.S., Aggarwal, N., Singh, R., 1990. Effects of cadmium and nickel on in vivo carbon dioxide exchange rate of pigeon pea (*Cajanus cajan* L.). *Plant Soil* 129, 243–249. <https://doi.org/10.1007/BF00032419>.
- Shimada, T.L., Hara-Nishimura, I., 2010. Oil-body-membrane proteins and their physiological functions in plants. *Biol. Pharm. Bull.* 33, 360–363. <https://doi.org/10.1248/bpb.33.360>.
- Shu, K., Yang, W., 2017. E3 ubiquitin ligases: Ubiquitous actors in plant development and abiotic stress responses. *Plant Cell Physiol.* 58, 1461–1476. <https://doi.org/10.1093/pcp/pcx071>.
- Singh, P., Arif, Y., Miszczuk, E., Bajguz, A., Hayat, S., 2022. Specific roles of lipooxygenases in development and responses to stress in plants. *Plants* 11, 979. <https://doi.org/10.3390/plants11070979>.
- Smeets, K., Ruytinx, J., Semane, B., Van Bellegem, F., Remans, T., Van Sanden, S., Vangronsveld, J., Cuypers, A., 2008. Cadmium-induced transcriptional and enzymatic alterations related to oxidative stress. *Environ. Exp. Bot.* 63, 1–8. <https://doi.org/10.1016/j.envexpbot.2007.10.028>.
- Soliman, M., Alhathloul, H.A., Hakeem, K.R., Alharbi, B.M., El-Esawi, M., Elkesh, A., 2019. Exogenous nitric oxide mitigates nickel-induced oxidative damage in eggplant by upregulating antioxidants, osmolyte metabolism, and glyoxalase systems. *Plants* 8, 562. <https://doi.org/10.3390/plants8120562>.
- Soltabayeva, A., Dauletova, N., Serik, S., Sandybek, M., Omond, J.O., Kurmanbayeva, A., Srivastava, S., 2022. Receptor-like kinases (LRR-RLKs) in response of plants to biotic and abiotic stresses. *Plants* 11. <https://doi.org/10.3390/plants11192660>.
- Song, A., Xue, G., Cui, P., Fan, F., Liu, H., Yin, C., Sun, W., Liang, Y., 2016. The role of silicon in enhancing resistance to bacterial blight of hydroponic- and soil-cultured rice. *Sci. Rep.* 6, 24640. <https://doi.org/10.1038/srep24640>.
- Stein, O., Granot, D., 2019. An overview of sucrose synthases in plants. *Front. Plant Sci.* 10, 95. <https://doi.org/10.3389/fpls.2019.00095>.
- Sun, Y., Huang, D., Chen, X., 2019. Dynamic regulation of plasmodesmatal permeability and its application to horticultural research. *Hortic. Res.* 6, 47. <https://doi.org/10.1038/s41438-019-0129-3>.
- Tóth, G., Hermann, T., Da Silva, M.R., Montanarella, L., 2016. Heavy metals in agricultural soils of the European Union with implications for food safety. *Environ. Int.* 88, 299–309. <https://doi.org/10.1016/j.envint.2015.12.017>.
- Vaculík, M., Pavlovič, A., Lux, A., 2015. Silicon alleviates cadmium toxicity by enhanced photosynthetic rate and modified bundle sheath's cell chloroplasts ultrastructure in maize. *Ecotoxicol. Environ. Saf.* 120, 66–73. <https://doi.org/10.1016/j.ecoenv.2015.05.026>.
- Vaculík, M., Kováč, J., Fialová, I., Fiala, R., Jašková, K., Luxová, M., 2021. Multiple effects of silicon on alleviation of nickel toxicity in young maize roots. *J. Hazard. Mater.* 415, 125570. <https://doi.org/10.1016/j.jhazmat.2021.125570>.
- Vandesompele, J., De Preter, K., Pattyn, F., Poppe, B., Van Roy, N., De Paep, A., Speleman, F., 2002. Accurate normalization of real-time quantitative RT-PCR data by geometric averaging of multiple internal control genes. *Genome Biol.* 3, research0034.1. <https://doi.org/10.1186/gb-2002-3-7-research0034>.
- Wood, B.W., 2015. Nickel. *Handbook of Plant Nutrition*.
- Wu, P., Gao, H., Liu, J., Kosma, D.K., Lü, S., Zhao, H., 2021. Insight into the roles of the ER-associated degradation E3 ubiquitin ligase HRD1 in plant cuticular lipid biosynthesis. *Plant Physiol. Biochem.* 167, 358–365. <https://doi.org/10.1016/j.plaphy.2021.08.021>.
- Xiao, R., Youngjun, O., Zhang, X., Thi, N.N., Lu, H., Hwang, I., 2023. Osmotic stress-induced localisation switch of CBR1 from mitochondria to the endoplasmic reticulum triggers ATP production via  $\beta$ -oxidation to respond to osmotic shock. *Plant, Cell Environ.* 46, 3420–3432. <https://doi.org/10.1111/pce.14671>.
- Xie, Z., Song, R., Shao, H., Song, F., Xu, H., Lu, Y., 2015. Silicon improves maize photosynthesis in saline-alkaline soils. *Sci. World J.* 2015, 245072. <https://doi.org/10.1155/2015/245072>.
- Xu, S., Lai, S.-K., Sim, D.Y., Ang, W.S.L., Li, H.Y., Roca, X., 2022. SRRM2 organizes splicing condensates to regulate alternative splicing. *Nucleic Acids Res.* 50, 8599–8614. <https://doi.org/10.1093/nar/gkac669>.
- Yang, C., Zhou, Y., Fan, J., Fu, Y., Shen, L., Yao, Y., Li, R., Fu, S., Duan, R., Hu, X., Guo, J., 2015. *SpBADH* of the halophyte *Sesuvium portulacastrum* strongly confers drought tolerance through ROS scavenging in transgenic *Arabidopsis*. *Plant Physiol. Biochem.* 96, 377–387. <https://doi.org/10.1016/j.plaphy.2015.08.010>.
- Zargar, S.M., Mahajan, R., Bhat, J.A., Nazir, M., Deshmukh, R., 2019. Role of silicon in plant stress tolerance: opportunities to achieve a sustainable cropping system. *3 Biotech* 9, 73. <https://doi.org/10.1007/s13205-019-1613-z>.
- Zhang, H., Shi, W.L., You, J.F., Bian, M.D., Qin, X.M., Yu, H., Liu, Q., Ryan, P.R., Yang, Z. M., 2015. Transgenic *Arabidopsis thaliana* plants expressing a  $\beta$ -1,3-glucanase from sweet sorghum (*Sorghum bicolor* L.) show reduced callose deposition and increased tolerance to aluminium toxicity. *Plant, Cell Environ.* 38, 1178–1188. <https://doi.org/10.1111/pce.12472>.
- Zhou, B., Yao, W., Wang, S., Wang, X., Jiang, T., 2014. The metallothionein gene, *TaMT3*, from *Tamarix androssowii* confers Cd<sup>2+</sup> tolerance in tobacco. *Int. J. Mol. Sci.* 15, 10398–10409. <https://doi.org/10.3390/ijms150610398>.



- Zhou, M.-X., Renard, M.-E., Quinet, M., Lutts, S., 2019. Effect of NaCl on proline and glycinebetaine metabolism in *Kosteletzkya pentacarpos* exposed to Cd and Zn toxicities. *Plant Soil* 441, 525–542. <https://doi.org/10.1007/s11104-019-04143-5>.
- Zhou, T., Xing, Q., Sun, J., Wang, P., Zhu, J., Liu, Z., 2024. The mechanism of *KpMIPS* gene significantly improves resistance of *Koeleruteria paniculata* to heavy metal cadmium in soil. *Sci. Total Environ.* 906, 167219. <https://doi.org/10.1016/j.scitotenv.2023.167219>.
- Zhu, G., Chang, Y., Xu, X., Tang, K., Chen, C., Lei, M., Zhu, J.-K., Duan, C.-G., 2019. EXPORTIN 1A prevents transgene silencing in Arabidopsis by modulating nucleocytoplasmic partitioning of HDA6. *J. Integr. Plant Biol.* 61, 1243–1254. <https://doi.org/10.1111/jipb.12787>.